processes

MDPI

*Review*

# Energy, Exergy, and Thermo-Economic Analysis of Renewable Energy-Driven Polygeneration Systems for Sustainable Desalination

**Mohammad Hasan Khoshgoftar Manesh [1,2,*] and Viviani Caroline Onishi [3,*]**

[1] Energy, Environment and Biologic Research Lab (EEBRlab), Division of Thermal Sciences and Energy Systems, Department of Mechanical Engineering, Faculty of Technology & Engineering, University of Qom, Qom 3716146611, Iran
[2] Center of Environmental Research, Qom 3716146611, Iran
[3] School of Engineering and the Built Environment, Edinburgh Napier University, Edinburgh EH10 5DT, UK
* Correspondence: M.Khoshgoftar@qom.ac.ir (M.H.K.M.); V.Onishi@napier.ac.uk (V.C.O.)

**Abstract:** Reliable production of freshwater and energy is vital for tackling two of the most critical issues the world is facing today: climate change and sustainable development. In this light, a comprehensive review is performed on the foremost renewable energy-driven polygeneration systems for freshwater production using thermal and membrane desalination. Thus, this review is designed to outline the latest developments on integrated polygeneration and desalination systems based on multi-stage flash (MSF), multi-effect distillation (MED), humidification-dehumidification (HDH), and reverse osmosis (RO) technologies. Special attention is paid to innovative approaches for modelling, design, simulation, and optimization to improve energy, exergy, and thermo-economic performance of decentralized polygeneration plants accounting for electricity, space heating and cooling, domestic hot water, and freshwater production, among others. Different integrated renewable energy-driven polygeneration and desalination systems are investigated, including those assisted by solar, biomass, geothermal, ocean, wind, and hybrid renewable energy sources. In addition, recent literature applying energy, exergy, exergoeconomic, and exergoenvironmental analysis is reviewed to establish a comparison between a range of integrated renewable-driven polygeneration and desalination systems.

**Keywords:** energy and exergy analysis; exergoeconomic analysis; exergoenvironmental analysis; economic analysis; renewable energy; sustainable development



**Citation:** Khoshgoftar Manesh, M.H.; Onishi, V.C. Energy, Exergy, and Thermo-Economic Analysis of Renewable Energy-Driven Polygeneration Systems for Sustainable Desalination. *Processes* **2021**, *9*, 210. https://doi.org/10.3390/pr9020210

Academic Editor: Julius Motuzas
Received: 28 December 2020
Accepted: 20 January 2021
Published: 23 January 2021



## 1. Introduction

Global energy and freshwater demands have risen hand-in-hand with population growth and economic development over the past decades. According to the International Energy Agency (IEA), significant progress has been achieved worldwide in increasing electricity access towards meeting the targets by 2030 [1]. Accordingly, the world's population lacking electricity access decreased from 1.2 billion in 2010 to 789 million in 2018 [2]. However, upholding this electrification rate will be challenging in the upcoming years due to the deficient distribution infrastructure and the difficulty of reaching isolated communities [3]. The implementation of decentralized polygeneration systems can be a suitable solution not only to address ever-increasing energy demands, but also to provide electricity to remote areas without requiring substantial investments in distribution infrastructures [3,4]. As far as water scarcity issue is concerned, integrating desalination technologies to conventional polygeneration systems can be considered for meeting freshwater demands, particularly in highly water-stressed countries. In this light, the most promising alternatives include the integration of the thermal and membrane desalination technologies such as multi-stage flash (MSF), multi-effect distillation (MED), humidification-dehumidification (HDH), and reverse osmosis (RO). Still, the urgency of achieving climate mitigation goals requires a

considerable increase of renewable energy shares in energy systems. Integrated renewable energy-driven polygeneration and desalination systems allow for mixing different renewable energy resources (e.g., solar, biomass, geothermal, ocean, and wind), while producing several useful energy services (including electricity, space heating and cooling, domestic hot water) and materials (freshwater, biofuels, synthetic fuels, and other chemicals). Figure 1 shows main inputs and outputs of typical polygeneration systems.

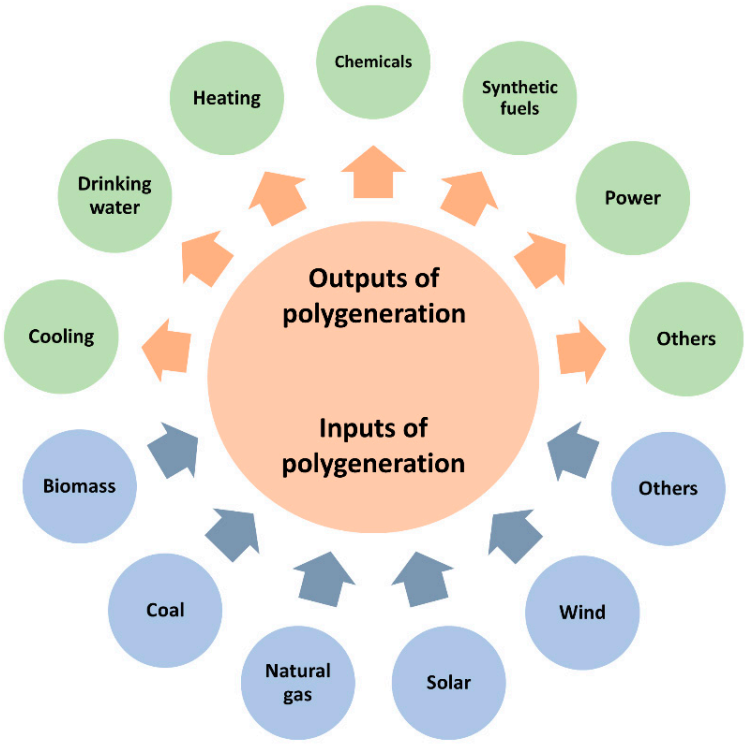


**Figure 1.** Schematic of inputs and outputs of typical polygeneration systems.

The appropriate design of an integrated renewable energy-driven polygeneration and desalination system leads to an optimized integration of distinct subsystems with the sharing of equipment between different processes, resulting in significant energy, costs, and environmental savings [5]. Nevertheless, the design and optimization of integrated renewable energy-driven polygeneration and desalination systems is a very complex endeavor, which requires advanced energy, exergy and thermo-economic-based tools to reliably improve the overall system performance. Within this framework, this review is designed to outline the latest developments on the modelling, design, simulation, and optimization of integrated renewable energy-driven polygeneration systems for sustainable desalination. Special attention is paid to the most innovative approaches focused on enhancing energy, exergy, and thermo-economic performance of decentralized polygeneration plants accounting for electricity, space heating and cooling, domestic hot water, and freshwater production, among others. Furthermore, recent literature applying energy, exergy, exergoeconomic, and exergoenvironmental analysis is reviewed to establish a comparison between a range of renewable-driven polygeneration systems.

This review is structured as follows. The most important thermal and membrane desalination technologies are presented in Section 2. Section 3 outlines the renewable energy resources used in polygeneration systems. The energy, exergy, and thermo-economic methodologies of analysis used in the literature are addressed in Section 4, while the latest works on renewable energy-driven polygeneration systems are discussed in Section 5. Finally, the major remarks and conclusions are summarized in Section 6.

## 2. Thermal and Membrane Desalination Technologies

Although the most crucial resource for sustaining life is water, accessible freshwater resources for human consumption are limited, consisting of only 0.75% of the Earth's available water. Approximately 97% of the global water resources is found as saline water in the oceans. A recent report from the United Nations [6] estimates that more than 2 billion people are currently living in highly water-stressed countries. It also highlights that around 700 million people in the world could be affected by 2030, if current degradation rates and unsustainable pressures continue to be exerted on natural water resources. The higher water-stressed countries are mainly located in Western Asia, Northern Africa, and Southern and Central Asia [7]. Drinking water from both surface and groundwater sources have been increasingly depleted over last decades, mainly due to the agricultural intensification, industrial production, urbanization, inadequate management, over-exploitation, pollution, and climate change [7,8]. Nevertheless, freshwater can be produced from the widely existing saline water through thermal and membrane desalination technologies as a viable solution to the water scarcity problem.

The global water demand is presently about 12.6 billion cubic meters per day, while the projections indicate an increase of 20% to 30% by 2050 [8]. Still, the world's current capacity for desalination is about 95 million cubic meters per day, which is twice the capacity of 44.1 million cubic meters per day in 2006 [9]. Seawater desalination (SWD) and brackish water desalination (BWD) account for 61% and 21% of global desalination capacity, respectively [10]. The desalination technologies can be categorized based on the feedwater (SWD or BWD), and the nature of the energy source utilized for driving the process (thermal, mechanical, or electrical) [11]. In line with the applied separation procedure, desalination technologies are also classified into thermal (phase-change based on evaporation and condensation phenomena) and membrane-based (non-phase change) separation processes. The most common thermal-driven technologies for SWD and BWD include MED, MSF, HDH, thermal vapor compression (TVC), and mechanical vapor compression (MVC) [12]. On the other hand, RO is a membrane-based technology with great importance in the global desalination market [13]. After the 1980s, the thermal-driven MSF and MED technologies have held a dominate market position accounting for about 84% of the global desalination capacity. However, this capacity has dropped to 50% by 2000 and 25% in 2019, of which 18% was related to MSF and 7% to MED. In 2019, the remaining 75% of the global desalination market was occupied by membrane-based RO desalination [14]. Figure 2 exhibits main thermal-driven desalination processes in which the utilization of waste heat is a remarkable benefit.

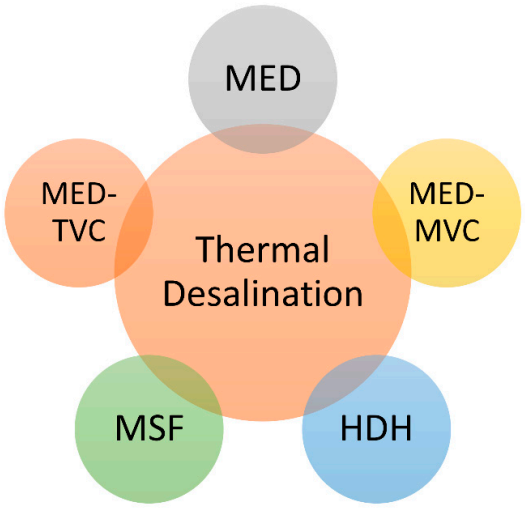


**Figure 2.** Classification of main thermal-driven desalination technologies. HDH, humidification-dehumidification; MED, multi-effect distillation; MSF, multi-stage flash; MVC, mechanical vapor compression; TVC, thermal vapor compression.

Thermal desalination is the most appropriate method for treating feedwater with high-salinity and temperature. Thermal desalination techniques are widely applied in the Middle East area due to its lower energy cost [15]. Nonetheless, major limitations for the broad implementation of important thermal and membrane-based desalination technologies are mostly related to their high thermal and electrical energy requirements, as well as the associated environmental impacts. For instance, RO needs large amounts of electricity to attain the high pressure conditions (55–82 bar) required for the SWD [16,17]. Several factors can affect the process recovery rate (i.e., freshwater production rate) such as the feedwater source, applied desalination technology, and other considerations for system design and configuration [18]. Thermal and membrane-based SWD have recovery rates of about 30% and 50%, respectively [15]. Yet, recovery rates can be as high as 75% to 90% for BWD by using membrane-based RO desalination [19]. The specific energy consumption, which is defined as the amount of energy per cubic meter of produced water, is up to 3.5 kWh-elec and 12 kWh-therm for MSF operating at >110 °C, and around 3.5 kWh-elec for RO [13]. The specific electrical and thermal energy consumption are 1.5 kWh-elec and 6 kWh-therm for MED operating at <70 °C [20].

The efficiency of thermal desalination systems can be described by the gain output ratio (GOR), defined as the freshwater production relative to the amount of steam consumed in the process [21]. Hence, the GOR is used to identify better opportunities in terms of capital and operating costs of different desalination units. Systems with greater GOR values present higher capital costs. However, they consume lower energy amounts and, therefore, have lower operating expenses. Thus, higher GOR values are usually considered in areas with high water demands. Systems with lower GOR values should be considered when the availability of low-value thermal energy is abundant [21].

Waste heat (WH) is known as a sustainable energy source with considerable capacity given that about half of the energy consumption in the world is currently wasted as WH [22]. Numerous processes that need thermal stimulation have used WH as a source of thermal energy [23]. The WH reclamation in a process can reduce the total energy consumption and, as a result, environmental impacts. In general, major WH sources in industries are liquid streams, steam, process gases and vapors, in addition to flue gases at temperature ranges of 50 to 300 °C, 100 to 250 °C, 80 to 500 °C, and 15 to 800 °C, respectively [23]. The WH is usually dissipated during the process as high-, medium-, or low-grade waste heat based on the temperature levels of >400 °C, 100–400 °C, and <100 °C, respectively [24]. One of the beneficial energy sources for desalination is the WH resulting from natural gas-compressor station (NG-CS). Approximately 60% of the energy input to compressor stations in the U.S. is wasted in the form of hot flue gases, which corresponds to an average of 610 TJ/d available from NG-CS at temperatures above 645 K [25,26]. Furthermore, low-grade heat can stimulate low-temperature boiling and evaporation, such as MED, HDH, and adsorption desalination (AD) [27].

There are many efforts toward decreasing the dependence of various industries on conventional fossil fuel energy due to climate change, global warming, and other environmental influences. In the desalination-related literature, several authors have attempted to employ renewable energy sources for powering distinct thermal and membrane processes [28]. Nevertheless, the intermittent nature of renewable energy production poses specific challenges on the system design and operation, particularly in terms of meeting the energy demands of the integrated system. For this reason, renewable energy-driven desalination usually requires applying energy storage for securing the supply of energy during downtime [29].

### 2.1. Multi-Stage Flash

Nowadays, MSF technology is being used in about 11% of the desalination plants throughout the world [30]. Once through (OT) and brine recirculation (BR) are the most common design configurations developed for MSF [31]. Although the first MSF plant configuration was based on the former configuration (MSF-OT), MSF-BR has become more

dominating because of lower operating expenses and fewer corrosion problems at large scales [32]. Currently, the situation has changed, and the progress in the field of corrosion protection and access to cost-effective anti-scalants have contributed to raise the number of MSF-OT plants worldwide [33].

The MSF-OT configuration is composed of two main parts, namely the brine heater (heat input) and flashing stages (heat recovery). First, saline feedwater is preheated by flowing through a set of tubes for heat exchange before entering the brine heater. In the latter, feedwater is heated utilizing the thermal energy resulting from low-pressure bleed steam (1–3 bars). It continues until the temperature reaches 90–110 °C, referred to as the top brine temperature (TBT) [34]. Afterwards, the previously heated saline water is led to the first stage in which the inner pressure of the brine heater is higher than the ambient pressure. The pressure decline results in saline water flashing. In this step, the flashing vapor condenses on the heat exchanger tubes, losing latent heat of condensation to the saline feedwater flowing inside the tubes. While distillate water is collected on a tray, the remaining saline water goes to the next step with lower pressure. The same procedure takes place repeatedly until the brine reaches the final stage and is discharged. Internal energy recovery could be increased by elevating the number of flashing stages [35]. The number of stages in a regular MSF desalination facility with capacity of 50,000 to 70,000 $m^3$/day ranges from 18 to 25 [36].

The lack of a system for controlling the inlet seawater temperature that alters in different seasons throughout the year is a major drawback for the MSF-OT configuration [37]. The elevated temperature of feedwater may reduce the total temperature difference (TTD). Moreover, a decline in the difference between the TBT and the temperature of inlet saline feedwater can decrease the production of freshwater in the plant [38]. The MSF-BR is beneficial for enhanced control over the feedwater temperature. This setting is composed of two sections, namely heat recovery and heat rejection. Heat recovery is similar to the MSF-OT flashing steps, in which the condensation latent energy is recovered. In the MSF-BR system, the inlet is the brine recycled from the final stage of the heat rejection part. The latent energy of formed vapors is absorbed by cooling SW and feed SW in this section, followed by the rejection of cooling SW back to the sea [39]. Intake SW volume and the steam needed for evaporation are diminished by brine recycle [35].

In a typical MSF configuration with a capacity of 50,000 to 70,000 $m^3$/day, the thermal energy demand varies from 190 MJ/$m^3$ (GOR = 12) to 282 MJ/$m^3$ (GOR = 8). The corresponding electrical energy consumed is equal to 15.83 kWh/$m^3$ and 23.5 kWh/$m^3$ by considering a power plant efficiency of 30% [17,40]. In addition, the MSF plant requires 2.5 to 5 kWh/$m^3$ of electrical energy for pumping [40]. As a result, the total equivalent energy used by a standard MSF unit ranges from 18.3 to 28.5 kWh/$m^3$ [40]. In order to develop new approaches for improving the process efficiency and decreasing energy requirements, it is necessary to understand energy usage and influential variables in MSF desalination. Numerous factors can affect the energy consumption in MSF, including the temperature difference between the heat source and heat sink, feedwater salinity in the flashing stages, geometrical configuration of flashing stages, construction materials, number of flashing stages, and heat exchanger area, among others [17]. Hence, the energy consumption of an MSF desalination plant can be decreased by adding flashing stages, and increasing the heat transfer area and the GOR [17]. Furthermore, scaling and fouling formation plays a remarkable role for affecting energy consumption and efficiency of MSF desalination. Deposits can be formed at high temperatures due to the presence of various types of salts, such as magnesium hydroxide, calcium carbonate, and non-alkaline scales [34]. Therefore, heat exchange is plugged by these deposits, leading to lower heat transfer rate and heat transfer efficiency. Consequently, scaling can also increase the operating costs [41]. In the next paragraphs, a discussion is presented on how changes in operating conditions and system configurations can influence process energy efficiency.

The TBT, defined as the temperature of saline feedwater before entering the flashing steps, is among the most critical operating parameters in MSF desalination. Higher TBTs

can increase the flash range, which leads to a higher freshwater production rate and enhanced energy performance [35]. Hanshik et al. [38] have investigated the impact of TBT augmentation on MSF-OT plant performance. The authors have performed theoretical calculations under the assumption of ideal conditions. Their results show that, although the TBT elevation increases the total energy consumption, less energy is needed for the production of one unit of freshwater. This is due to higher freshwater production rates achieved in the proposed process. Their results also reveal that process costs can be reduced by rising the TBT. However, they conclude that scaling-related problems can limit the MSF plant extension by the TBT elevation approach.

Some changes in the plant configuration may also enhance the energy efficiency of the MSF desalination process. In this regard, Hamahmy et al. [42] have assessed a modification of an MSF-OT setting named brine extraction. In this process, part of the cooling brine is extracted from upper parts of the system and then, directly reinjected into flashing chambers of the down stages. This system modification demands extra piping since the extracted brine is not preheated before reinjection. While their modelling approach allows investigating single and multiple-point extractions of brine, the results show that the former is more suitable due to relative configuration simplicity and improved performance. Still, the energy consumption in MSF can be greatly affected by the arrangement of the heat exchanger tubes. Applying a long-tube arrangement instead of a cross-flow one can assist in saving the power required by the SW supply pump. This is owed to the pressure drop in the heat exchanger tubes. However, most of the commercial MSF plants are based on a cross-flow configuration [43]. The use of long-tube arrangement is limited because of its higher leakage probability and space constraints, since tubes with several hundred meters might be required under this configuration [38].

MSF is a very mature desalination technology that has been utilized since the 1960s [44]. Studies on the enhancement of MSF process energy efficiency still concentrate on optimizing operating conditions or modifying process configurations. Nonetheless, these enhancements are mostly evaluated via modelling approaches or theoretical energy calculations, which are not sufficient for assessing the energy performance of real systems. Therefore, advanced approaches based on both energy and irreversible thermodynamic losses are required to more accurately evaluate the effects of these improvements on optimal system performance.

### *2.2. Multi-Effect Distillation*

MED is one of the oldest desalination technologies and had significant scaling issues in the initial development stages. In the 1960s, MSF replaced MED due to its ability to present fewer scaling issues [44]. On the other hand, MED usually presents lower thermal energy demands than MSF [45]. This is because the water boiling in MSF needs elevated amounts of high-temperature steam at TBT close to 100 °C. In contrast, the water boiling in MED occurs at the lower temperatures of 70 to 90 °C since the operating pressure is lower than the atmospheric pressure [21]. As a result, MED uses less steam than MSF for producing the same volume of freshwater [35].

MED technology mainly consists of a condenser and multiple distillation effects. In summary, saline feedwater is firstly preheated in the condenser tubes. Then, warm feedwater usually flows to the multiple effects in equal proportions. In each distillation effect, saline feedwater is sprayed onto the outer surface of evaporator tubes. In the first effect, the water sprayed onto the evaporator tubes absorbs heat from the low-pressure steam in the tubes and vaporizes. Steam is condensed by losing energy to the saline water. Vapor resulting from feedwater evaporation is used as the energy source to the successive effects, while the vapor from the last effect is utilized to preheat saline feedwater in the condenser. Thus, the vapor is condensed yielding to freshwater [36]. In MED, the external steam is exclusively supplied in the first stage, whereas in the remaining ones the energy removed by cooling is used as an energy source for heating subsequent effects. This is carried out by decreasing the pressure in each successive stage.

The amount of freshwater produced in the MED process has a direct relationship with the number of effects. In this way, freshwater production rates increase as the number of effects is augmented in the process. Nevertheless, the number of effects is controlled by the minimum allowable temperature difference between successive effects, along with the total temperature range available in the process [21,46]. The number of effects in MED usually ranges from 4 to 21, which is dependent on the heat source and top brine temperatures (typically around 70 to 90 °C) in the first effect [17,21]. Similarly to MSF, MED also requires thermal (low-temperature heat for evaporation) and electrical energy (electricity for pumps) sources. Typical MED plants with a capacity of 600 to 30,000 $m^3$/day consume about 145 MJ/$m^3$ (GOR = 16) to 230 MJ/$m^3$ (GOR = 10) of thermal energy. In these plants, the corresponding electrical energy ranges from 12.2 to 19.1 kWh-elec/$m^3$ based on power plant efficiencies of 30% [17]. Furthermore, 2 to 2.5 kWh/$m^3$ of electrical energy is used in MED for pumping. Therefore, the total specific energy consumption in a typical MED plant ranges from 14.45 to 21.35 kWh-elec/$m^3$ [17]. The specific energy consumption of MED is affected by the same factors as MSF. Thus, the MED performance is influenced by changes in operating conditions and system configuration, including the flow arrangement of the feedwater and vapor.

In MED, feedwater is supplied to the effects as three different configurations, namely forward feed, backward feed, and parallel feed [47]. The flow direction of brine and vapors is the major difference between these arrangements. In the forward feed scheme, all the feedwater is heated in the first effect resulting in a vapor, which is used to heat the next effects. In this case, flows of feed and vapor are in the same direction. In the backward feed scheme, saline feedwater and vapor follow opposing directions and enter the low-temperature end high-temperature effects, respectively. As a result, the high-salinity water is in contact with the high-temperature effect. The brine flows from the high-pressure effect towards the low-pressure one. Therefore, additional pumping is required between the steps in this arrangement. Moreover, the setting is vulnerable to severe scaling. Al-Mutaz and Wazeer [48] have performed a parametric study on diverse MED arrangements via mathematical modelling approaches. The authors have investigated the impact of a variety of parameters on MED performance. Their results demonstrate that the specific heat transfer area increases with the number of effects in all configurations. This is because an increase in the number of effects diminishes the temperature drop per effect, when the total temperature of the process is constant. Consequently, more heat transfer area is needed for keeping water production at a determined level.

A limitation of MED technology is related to the need for sizeable specific heat transfer areas in comparison with MSF [21]. Morin [49] has demonstrated that MED requires almost double of the heat transfer area needed by a similar MSF system. The heat transfer area can be reduced in MED plants by operating at higher TBT. This is because lower temperatures are associated with smaller heat transfer coefficients. Although MSF is the most frequent thermal technology throughout the world, it generally requires more energy and higher capital costs when compared to MED. The integration of MED with a solar power plant is promising, and several authors have focused on solar-assisted MED systems [50]. Solar-driven MED technology has been increasingly popular in the Arab states of the Persian Gulf [51] due to the abundance of solar energy in these regions. Furthermore, MED can operate at low temperatures, making it suitable for utilization with low-temperature sources, including geothermal energy and WH [52]. The coupling of MED with TVC or MVC can improve the energy performance and capacity of the process. Currently, the capacity of commercial MED-TVC and MED-MVC plants are 70,000 to 80,000 and <10,000 ton/d, respectively. Combining MED with TVC and MVC can reduce the consumption of thermal energy by taking advantage of the vapor from the last effect [53].

Several authors claim that the implementation of MSF will continue to grow and develop in the future [54]. Some other authors believe that the number of MED plants will increase over time, while the installed capacity of MSF will remain high [55]. Although MED is a suitable technology that presents lower energy demands than MSF, the research on this area is also mainly focused on improving operational conditions or process configurations via energy calculations based on the first law of thermodynamics. Hence, advanced approaches combining energy and exergy analyses are needed to more precisely assess the effects of different process conditions and configurations on the optimal performance of real MED systems.

### *2.3. Humidification-Dehumidification*

HDH desalination systems are mainly composed of two main components: the humidifier and the dehumidifier units. The schematic diagram of a typical HDH desalination process is depicted in Figure 3. A variety of energy sources can be used to power the HDH systems. The HDH process is based on the natural desalination cycle (or rain cycle), in which the solar energy heats the seawater. In the rain cycle, the evaporation of seawater to the atmosphere leads to clouds formation followed by rain due to air dehumidification at elevated sea levels. Thus, HDH is an artificial version of the mentioned cycle [56]. The air capability for carrying moisture is the principle behind the HDH desalination system. Hence, the air stream enters the humidifier section and absorbs moisture from saline water. Then, the freshwater is produced from the humid air in the dehumidifier unit. In this process, the saline water is diffused into the air stream in the humidifier unit owed to the difference of water vapor concentration between the air and water vapor interface.

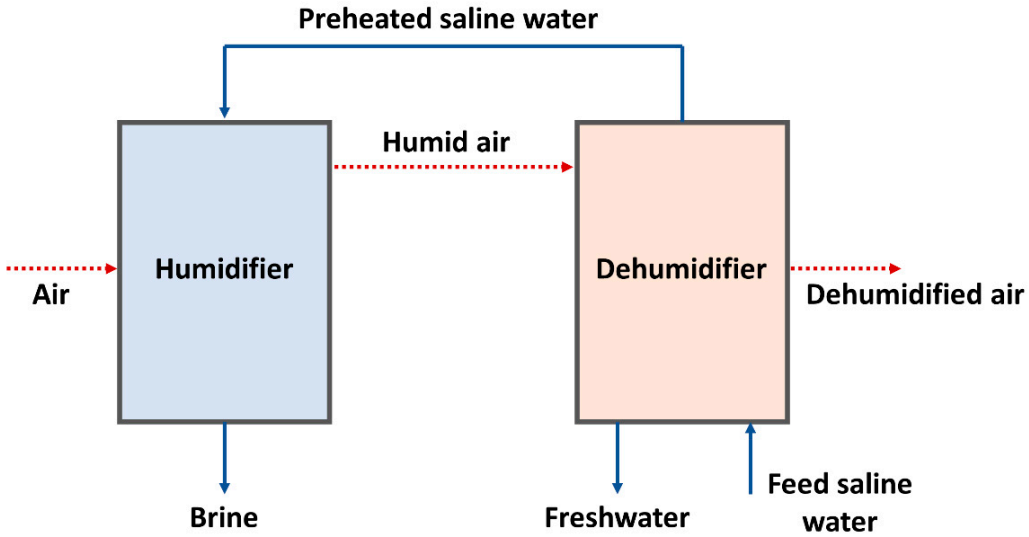


**Figure 3.** Schematic diagram of a typical humidification-dehumidification (HDH) desalination process.

The diffusion process increases moisture contents in the saturated air, as well as the brine salinity at the discharge of the humidifier unit. The saturated air preheats the saline feedwater in the dehumidifier section, while freshwater is condensed from the humid air [56]. There are three different HDH system configurations, namely closed-air open-water (CAOW), open-air closed-water (OACW), and open-air open-water (OAOW) cycles. The systems can also be categorized according to the streams being heated in the process as water-heated-(WH) and air-heated-(AH)-HDH. Considerable research has been performed towards improving the performance of HDH desalination systems. Thus, a number of authors have investigated different system configurations and types of humidifier/dehumidifier equipment via either theoretical or experimental approaches [57,58]. In this regard, packed-bed humidifiers are the most common types of humidifiers used in these studies, whereas direct-contact dehumidifiers are the preferable choice due to

their improved performance [56]. Several works have also focused on improving system performance by using low-grade heat and renewable energy sources, including biomass, geothermal, solar photovoltaic, to name but a few. Recently, Xu et al. [59] have shown that the energy performance of solar-assisted HDH systems can be considerably improved by increasing the temperature of the saline feedwater (seawater). Faegh et al. [56] have presented a comprehensive review on HDH desalination systems coupled with power, refrigeration, and desalination technologies. The authors have highlighted the potential performance enhancement of HDH systems through their integration with heating and cooling loads of refrigeration systems, Kalina and Rankine power cycles, and other desalination technologies such as MED and RO.

### *2.4. Reverse Osmosis*

RO is a membrane-based desalination technology that is well-known as a reliable state-of-the-art process for producing freshwater from both SWD and BWD. RO desalination is a non-phase change operation, which is characterized as a pressure-driven process. In the RO desalination process, the dissolved salts are removed from a high-pressure saline feedwater stream via a semi-permeable membrane [21]. The flow across the membrane is driven by a pressure difference between the high-pressure saline feedwater and the low-pressure distillate. Thus, the water molecules move from the region of high salt concentration to the low region owed to the osmotic pressure. Consequently, the pressure of the saline feedwater needs to be increased to a pressure higher than the osmotic one, whereas the distillate is maintained at near-atmospheric conditions [60]. RO desalination systems are usually composed of a pre-treatment unit, a high-pressure pump, a membrane unit, and a turbine or a valve, as depicted in Figure 4 [17,61]. The pre-treatment methods employed mostly depend on the type and configuration of the membrane, recovery ratio, freshwater quality requirements, and feedwater characteristics. The major pre-treatment methods include acid addition, filtration, dichlorination, and coagulation, to name but a few. The pre-treatment is used to remove contaminants from the feedwater such as bacteria, large, suspended solids, and colloidal matter that might impair the membrane operation [21]. In addition, cleaning solutions can be used as pre-treatment to avoid fouling and scaling problems. The high-pressure pump produces the elevated pressures required to drive the process. The operating pressures of 17 to 27 bars are related to BWD, while SWD usually requires around 55 to 82 bars for desalination [17]. Some RO systems also include a post-treatment unit to adjust the pH and remove gases such as hydrogen sulfide [17].

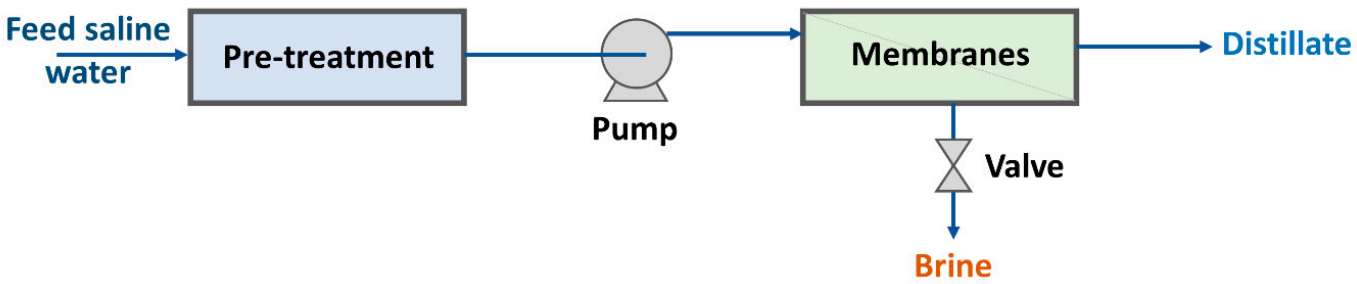


**Figure 4.** Schematic diagram of the reverse osmosis (RO) desalination system as proposed by Amidpour and Khoshgoftar Manesh [61].

RO plant capacities can vary from very small sizes of 0.1 $m^3$/day (household applications) to as large ones as 395,000 $m^3$/day (industrial applications) [17]. The average energy consumption reported in the literature ranges from 3.7 to 8 kWh/$m^3$ [17]. The energy consumption is mainly associated with the electricity needed to drive the high-pressure pump for the saline feedwater pressurization, along with the energy required for pre-treatment process. However, the energy consumption required for pumping is highly dependent on the feedwater salt concentration. In this way, higher amounts of

energy are required for high-salinity feedwaters as a result of the higher osmotic pressures required in the process [21]. Therefore, a RO plant for SWD requires large amounts of energy than one for BWD with the same capacity [46]. A typical RO unit used for SWD with production capacity of 24,000 $m^3$/day presents an energy consumption ranging from 4 to 6 kWh/$m^3$. Since lower pressures are required for BWD, the electrical energy consumption of a brackish water RO unit varies from 1.5 to 2.5 kWh/$m^{3.}$ [17]. Freshwater recovery ratios for RO desalination ranges from 25 to 45% for seawater and up to 90% for brackish water [62]. The separation efficiency of the RO process is severely affected by membrane scaling and fouling. However, these issues can be reduced or even avoided by applying effective pre-treatments and using anti-scalants. RO is a mature technology and considerable research has been performed over the last decades to improve its overall energy performance. As a result, the energy consumption of the RO technology has been considerably reduced since the 1970s. A number of factors have contributed to the latter achievement, including membrane technology development, improvements on pumping efficiency, and the implementation of energy recovery units [63].

## 3. Renewable Energy Resources

In recent years, polygeneration and desalination systems based on renewable energy resources have attracted increasing interest because of its innumerable benefits. The major advantages of using renewable energy in polygeneration and desalination include reducing the dependence on fossil fuels and the related carbon emissions. The primary renewable energy resources are listed as solar, wind, hydropower, biomass, geothermal, and ocean energy, as depicted in Figure 5. However, the very stochastic and intermittent nature of renewable energy generation hinders the energy management and practical operation of renewable energy-based polygeneration and desalination systems (and the integrated systems combining both). Moreover, it should be observed that not all renewable energy resources are advantageous for all polygeneration or desalination systems. Some renewables are more beneficial for small-scale plants rather than large-scale ones [64]. Several factors should be considered while choosing a renewable energy resource, including energy accessibility, local weather conditions, available infrastructure, and governmental regulations. The use of biomass to produce energy, for instance, can be quite controversial in some countries, mainly due to its correlation to food production and land-use. Thus, it should be considered only on sustainable levels that do not impair other societal sectors [65]. Given its abundance throughout the globe, solar energy usage is of particular interest in integrated polygeneration and desalination systems. Figure 6 shows the most important solar energy technologies, auxiliary resources, and possible outputs of solar-driven polygeneration systems.

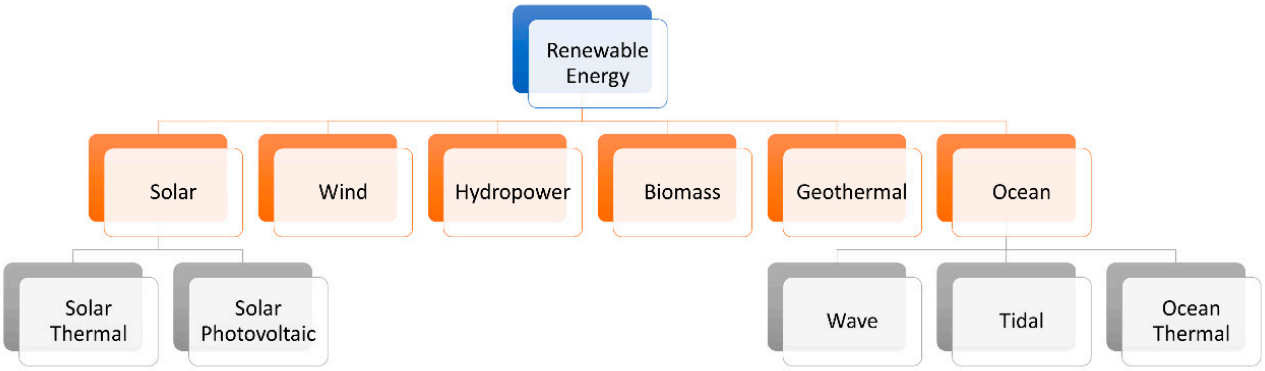


**Figure 5.** Classification of main renewable energy resources.

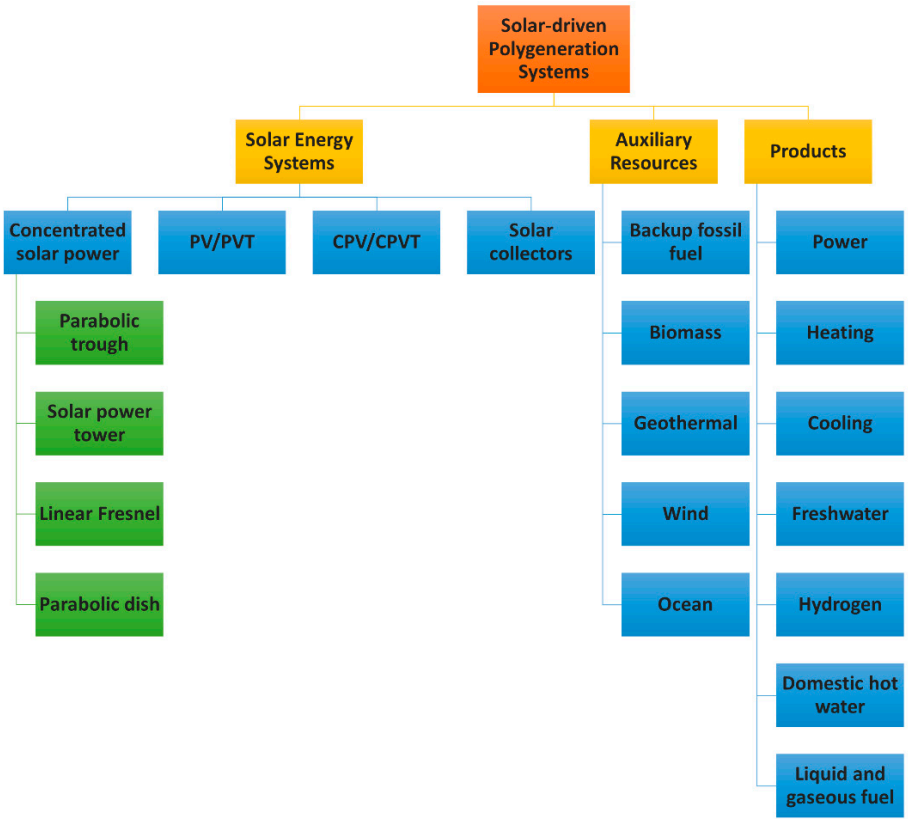


**Figure 6.** Solar-driven polygeneration systems [64]. CPV, concentrated photovoltaic; CPVT, concentrated photovoltaic thermal; PV, photovoltaic; PVT, photovoltaic thermal.

## 4. Energy, Exergy, and Thermo-Economic Analyses of Integrated Systems

Energy, exergy, and economic aspects are all important to evaluate the performance as well as to optimize integrated polygeneration and desalination systems [65]. Numerous approaches have been proposed in the literature for the analysis of cogeneration, polygeneration, and desalination systems. These approaches include the thermodynamic modeling, simulation, and/or optimization of the entire system [66–69]. However, studies centered only on improving operating conditions or modifying process configurations via theoretical energy calculations may not suffice to describe the performance of real systems. Instead, comprehensive thermodynamic investigations should be carried out on the whole system, including mass, energy, and exergy balances, along with the determination of energy and exergy efficiencies, and the economic performance assessment.

The first law of thermodynamics provides a suitable estimation of energy demands in polygeneration and desalination processes [70]. However, the energy demand estimated theoretically by this law and that from practical settings can be significantly different. The difference is mainly associated with the irreversible losses of real processes. Hence, advanced tools able to simultaneously address both the quantity and quality of energy can offer a more realistic assessment of the required energy consumption. In this way, exergy analysis can be used for examining the performance of energy systems [71]. Exergy is defined as the maximum useful work obtained when a system changes from the initial to the state of equilibrium with the environment [72].

The exergy efficiency characterizes the performance of a system or a component from a thermodynamic point of view, by computing the ratio of useful work output to the reversible one. It basically allows to assess the system effectiveness against its performance under reversible conditions. For this reason, exergy analysis can present a better understanding of the energy losses in polygeneration and desalination processes by determining the sites of irreversible losses [72]. Yet, exergy destruction determination is complicated

and requires knowledge of the thermodynamics of working fluids. Nevertheless, the application of the first and second laws of thermodynamics allied with either environmental or economic (or both) performance aspects provides a very powerful analysis tool to enhance integrated polygeneration and desalination systems.

Distinct approaches are available in the pertaining literature for formulating exergy and energy efficiency in polygeneration and desalination plants [63]. Energy, exergy, and thermo-economic related performance parameters can also be applied as objective functions in optimization approaches [73]. In addition, the application of combined energy, exergy, exergoeconomic, and exergoenvironmental analysis, known as 4E-analysis, allow for better understanding of the interactions between different systems components. The flowchart for the energy, exergy, exergoeconomic, and exergoenvironmental (4E) analysis is presented in Figure 7.

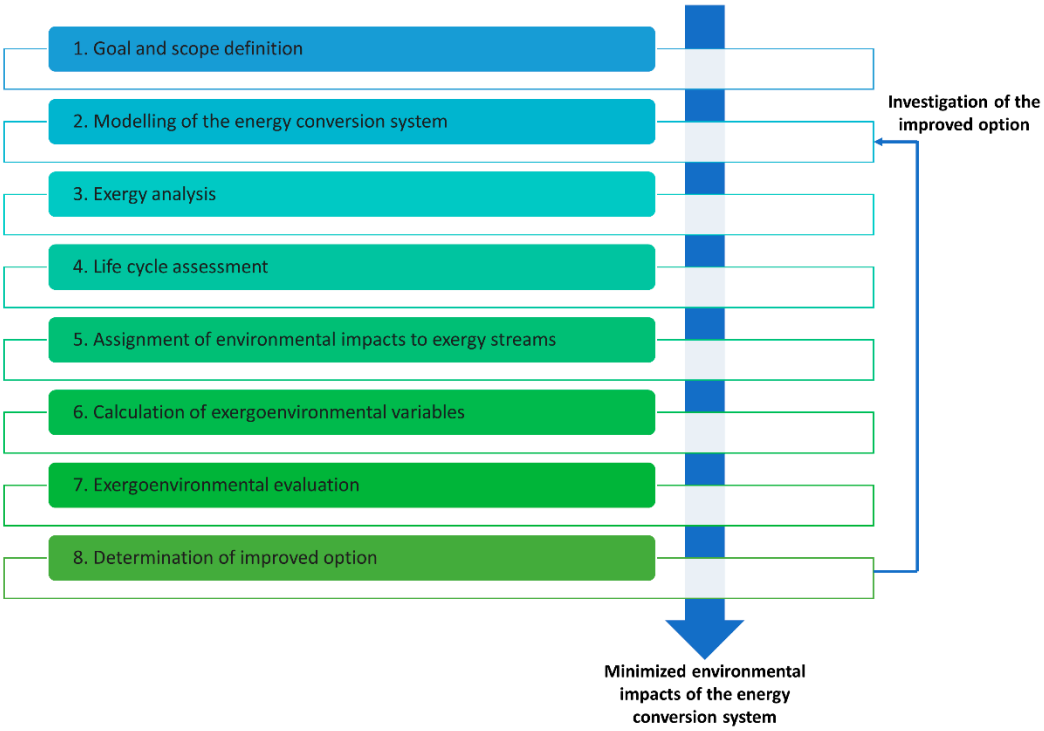


**Figure 7.** Flowchart of energy, exergy, exergoeconomic, and exergoenvironmental (4E) analysis.

## 5. Renewable Energy-Driven Polygeneration Systems

### *5.1. Integrated Polygeneration and MSF Desalination Systems*

Hogerwaard et al. [74] have proposed a polygeneration system that integrates a solar-driven gas turbine to an organic Rankine cycle (ORC), a single-effect absorption refrigeration system (ARS) with cold thermal energy storage (TES), flash desalination, and direct space heating. Thus, the outputs of the polygeneration system include space cooling and heating, freshwater, and domestic hot water (DHW). In this system, air is generated in the gas turbine inlet at a temperature of 1000 °C by three concentrated solar collectors with rated concentration ratios of 300, 500, and 800 at the solar insolation of 800 W/m$^2$. The authors have contrasted the proposed polygeneration system with a reference system composed of the same solar system with a Kalina power cycle at exergy and energy efficiencies of 0.29 and 0.275, respectively. Their results reveal that the polygeneration system yields to similar exergy and energy efficiencies of 0.27 and 0.284, respectively. Even though the exergy and energy efficiencies of both systems are comparable, the solar-assisted polygeneration system proposed by the authors offers an additional commodity production from a single-heat source for community level or small commercial applications. Hence,

their system constitutes a more sustainable alternative since it does not require any extra primary energy resources.

Azhar et al. [75] have studied an integrated renewable energy-driven polygeneration and desalination system able to simultaneously generate electrical power, space cooling, industrial heating, and freshwater. The integrated system is powered by a hybrid renewable energy generation plant composed of ocean thermal energy conversion (OTEC), solar collectors, and geothermal energy system as a backup for solar energy given its intermittent nature. Thus, their polygeneration system integrates concentrated solar collectors, steam turbines, heat exchangers, condenser, cooling tower, steam separator, mixing chamber, pumps, and expansion valves. In addition, an MSF desalination plant is used to produce freshwater from seawater, whereas a direct steam generator (DSG) is applied to power production from solar energy. Their results show that the OTEC system achieves a power production of 30.49 kW and an energy efficiency of 0.73%, when coupled to the MSF desalination plant. In addition, the MSF plant produces 18.54 kg/s of freshwater with 51.58% of energy efficiency, while 39.48 MW of thermal energy are provided for industrial heating by polygeneration.

Sezer and Koç [76] have assessed the performance of an integrated polygeneration system based on solar, wind, and osmotic power according to the first and second thermodynamic principles. Their proposed system encompasses concentrated photovoltaic/thermal (CPVT) panels, TES unit, wind turbines, hydrogen fuel cell and electrolyzer, vapor compression refrigeration (VCR) cycle, pressure retarded osmosis (PRO), and MSF unit for seawater desalination, as shown in Figure 8. The system is designed to produce several useful commodities, including electricity, freshwater, hydrogen, oxygen, and refrigeration. Moreover, the authors have performed a comprehensive parametric study to evaluate the effects of changing operating and environmental conditions together with other input parameters on production rates, exergy destruction rates, and energy and exergy efficiencies. After analyzing the integrated system thermodynamically, their results show overall energy and exergy efficiencies of 73.3% and 30.6%, respectively. In summary, the authors have successfully established that the production of multiple commodities can be guaranteed through combining multiple renewable energy resources along with efficient energy conversion and storage.

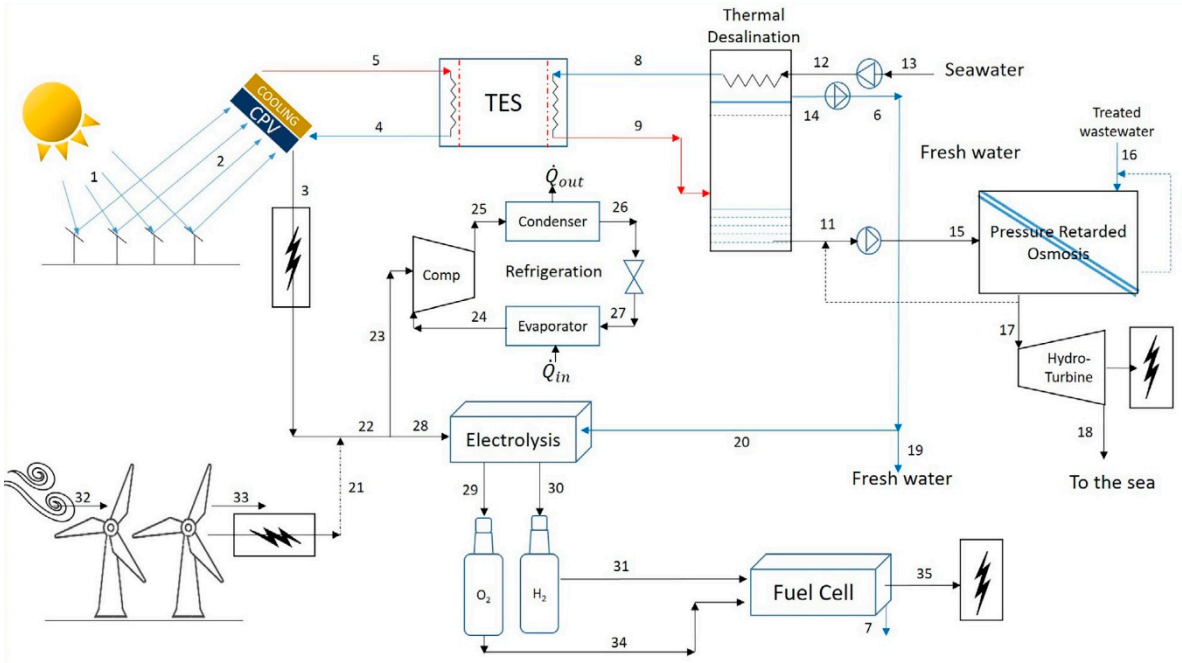


**Figure 8.** Schematic diagram of the multigeneration system proposed by Sezer and Koç [76]. CPV, concentrated photovoltaic; TES, thermal energy storage.

Luqman et al. [77] have investigated a sustainable decentralized renewable energy-aided polygeneration system for remote locations via thermodynamic analysis. The integrated system proposed by the authors include the following equipment: concentrated solar power (CSP), water electrolyzer, food drying system, Rankine cycle, oxy-hydrogen combustor, domestic water heater, wind turbine, refrigeration unit, hydrogen and oxygen storage units, and MSF desalination unit. Besides, a TES unit and an oxy-hydrogen combustion unit are incorporated to the system for ensuring continuous plant operation overnight and under cloudy weather conditions. Hence, their system is able to uninterruptedly produce electricity, cooling, hydrogen, oxygen, food drying, DHW, and freshwater from seawater desalination. The results from the reference case demonstrate that under the installation of parabolic trough concentrators (PTCs) with total area of 111,728 $m^2$, the integrated system generates ~11.4 MW of net electrical power, ~828 $m^3$/day of freshwater, 920 kg/day of $H_2$, ~36 kg/s of hot air for food drying, ~2.26 MW of cooling, and ~31 kg/s of DHW. The overall energy and exergy efficiencies of the integrated system are found to be 50% and 34%, respectively. Furthermore, their results reveal that the energy efficiency is equal to ~15%, while the exergy efficiency is ~16%, when considering a single generation plant in which the only output is electrical power. Therefore, their findings highlight the advantages of implementing integrated renewable energy-driven polygeneration systems in remote locations.

Recently, Luqman et al. [78] have thermodynamically evaluated a solar-driven polygeneration system for sustainable desalination. Their proposed system is composed of solar PTCs that are employed to power the MSF desalination plant. The authors consider the integration of a PRO system to reduce the salinity of brine discharges from the MSF unit, as well as to generate additional electrical energy. Moreover, an ORC unit is used to produce electricity, while recovering the waste heat from desalination. An absorption cooling system (ACS) is also integrated to the system to provide cooling and recover the waste heat from the brine. Finally, a TES unit is used for ensuring continuous operation at nighttime. In their study, the authors have carried out a thorough thermodynamic analysis via energy, exergy, entropy, and mass balances, and assessment of overall energy and exergy efficiencies of the system. Their results show that the integrated polygeneration and desalination system produces 583.3 kW of electricity, ~4284 kW of cooling, and 1140 $m^3$/day of freshwater under reference conditions and a total PTCs area of 100,000 $m^2$. Still, under the designed conditions, the overall system energy and exergy efficiencies are 34.54% and 14.55%, respectively. Therefore, their findings also emphasize the ability of decentralized renewable energy-driven polygeneration systems to effectively produce several commodities for addressing energy and water demands of remote communities.

Luqman and Al-Ansari [79] have proposed a hybrid solar-biomass polygeneration system to simultaneously provide electricity, freshwater, DHW, space cooling, as well as cooling for food storage, and hot air for food drying. Their polygeneration system consists of a Rankine Cycle, a CSP system, an MSF desalination unit, an ACS, and a biomass combustor. The authors have performed a thermodynamic analysis of the decentralized system to maximize the outputs production, while improving the system resilience under distinct weather conditions and day/night operating cycles. Thus, the authors have developed an integrated thermodynamic model based on energy, exergy, entropy, and mass balances. In addition, they have investigated how different environmental conditions affect the process dependent variables and performance. Their results reveal overall energy and exergy efficiencies for the integrated system of 55% and 18%, respectively. Under the latter conditions, the system outputs include ~4 MW of cooling, ~13 MW of electricity, ~41 kg/s of DHW, ~73 kg/s of hot air for food drying, along with 1687 $m^3$/day of freshwater. Besides, their results show that the biomass combustion unit and PTCs system have the highest exergy destruction levels in the system. Therefore, their decentralized renewable energy-driven polygeneration system can potentially address several energy and water demands from a coastal community. Table 1 presents the summary of topical research on renewable energy-driven polygeneration systems based on MSF desalination.

**Table 1.** Summary of topical research on integrated renewable energy-driven polygeneration and MSF desalination systems.

| Reference | Methodology | Products | Renewable Energy Source | Main Observations |
|---|---|---|---|---|
| Hogerwaard et al. [74] | Thermodynamic and exergy analysis | Power, cooling, heating, and freshwater | Solar | - Concentrated solar collectors<br>- Performance comparisons of polygeneration system with stand-alone system<br>- Use of renewable energy to improve sustainability |
| Azhar et al. [75] | Thermodynamic and exergy analysis | Industrial heating, space cooling, electrical power, and freshwater | Solar, geothermal, and ocean thermal energy | - Integrated polygeneration system using renewable energies<br>- Energy and exergy efficiencies are calculated<br>- Power generation of 30.49 kW<br>- Energy efficiency of 13.93%<br>- Exergy efficiency of 17.97% |
| Sezer and Koç [76] | Thermodynamic and exergy analysis | Hydrogen, oxygen, desalted water, refrigeration, and electricity | Solar, wind, hydrogen, and osmotic power | - For cooling of photovoltaics, the boiling heat transfer is evaluated<br>- Comprehensive performance and parametric investigations are performed over the system<br>- Elimination of impact of brine discharge on the marine environment |
| Luqman et al. [77] | Thermodynamic and exergy analysis | Freshwater, electricity, cooling, hydrogen, and oxygen | Solar and wind | - Use of $H_2$-$O_2$ combustor and TES for stable operations<br>- Overall energy efficiency of 50%<br>- Overall exergy efficiency of 34% |
| Luqman et al. [78] | Thermodynamic and exergy analysis | Electricity, freshwater, and cooling | Solar PTC with TES | - Overall PTCs area of 100,000 $m^2$<br>- The system generates 583.3 kW of electricity, 4284 kW of cooling, and 1140 $m^3$ of desalinated water per day<br>- Overall energy efficiency of 34.54%<br>- Overall exergy efficiency of 14.55% |
| Luqman and Al-Ansari [79] | Thermodynamic and exergy analysis | Electricity, freshwater, hot water, and food storage | Solar and biomass | - The system promotes a decentralized EWF nexus approach in coastal communities<br>- Overall energy efficiency of 55%<br>- Overall exergy efficiency of 18% |

Abbreviations: EWF, Energy-Water-Food; MSF, multi-stage flash; PTC, parabolic trough collectors; TES, thermal energy storage.

### *5.2. Integrated Polygeneration and MED Desalination Systems*

Abdelhay et al. [80] have examined the thermo-economic aspects of a polygeneration system consisting of a SPS, an ARS, and a MED desalination unit. The proposed plant is driven by solar PTCs, and a natural gas-fired heater is used as backup energy source. Figure 9 displays the schematic diagram of the integrated polygeneration plant as proposed by the authors. The authors have performed a detailed plant simulation using MATLAB software. They have also carried out a parametric analysis to assess the effects of varying different operating and design parameters on the overall system energy and exergy efficiencies. Finally, they have completed an economic evaluation in terms of capital investment and operating expenses. Their results demonstrate that the proposed integrated system could lead to the lowest unit water price (1.247\$/$m^3$) and unit cooling price (0.003\$/kWh), as well as the highest exergy efficiency (23.95%), in comparison with the single and dual-purpose ARS-MED systems.

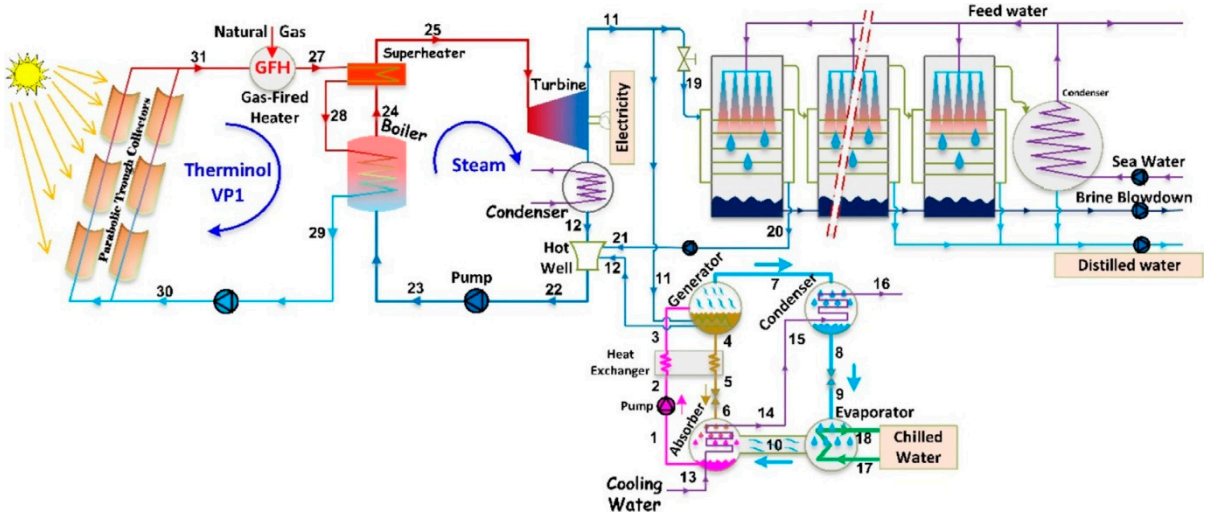


**Figure 9.** Schematic diagram of the integrated polygeneration plant proposed by Abdelhay et al. [80]. The plant is composed of a solar power system (SPS), multi-effect distillation (MED), and an absorption refrigeration system (ARS).

The integration of evacuated tube solar collectors (ETC) with a polygeneration and MED desalination system has been studied by Calise et al. [81]. The authors have proposed an optimization and dynamic analysis of the solar-driven polygeneration designed to produce heating, cooling, and freshwater. The thermo-economic analysis has been performed by considering a polygeneration plant comprised by a MED unit for seawater desalination, a single-effect water-lithium-bromide absorption chiller (ACH) unit, a backup biomass heater, balance-of-plant devices, heat exchangers, and tanks. The authors have developed a zero-dimensional dynamic simulation model using the TRNSYS software under different strategies to control the system. Their results show a payback period of approximately 3.5 years. On the other hand, their optimization method based on Design of Experiment (DoE) presents a payback period of 2.4 years, by setting the total area of the solar collector's field equal to 1200 $m^2$, along with summer/winter outlet temperatures of 95 °C/50 °C, and the tank dead band temperature of 2 °C.

Vazini and Khoshgoftar Manesh [82] have evaluated the power, heating, and freshwater production in a setting located in Qeshm Island, Iran. In their study, the polygeneration system is composed of a MED-TVC/RO desalination, a gas turbine unit, an ACH unit, and solar parabolic trough collectors. The authors have performed comprehensive exergy, exergoeconomic, and exergoenvironmental analyses of a solar-based polygeneration system. Their methodology is based on multi-objective genetic algorithm (MOGA), and multi-objective water cycle algorithm (MOWCA). They have concluded that setting the inlet air in the cooling system up to the gas cycle temperature allows for reducing unwanted impacts on the environmental conditions. Moreover, the integration of the MED unit with the RO desalination system, together with the solar thermal collectors improves the overall system performance.

Calise et al. [83] have carried out a dynamic thermo-economic analysis of integrated solar-biomass polygeneration and desalination systems. They have evaluated the integration of two distinct solar thermal technologies into a polygeneration plant, namely ETC and linear Fresnel reflector (LFR). The first plant layout embraces a single-effect water-lithium-bromide ACH unit, a biomass auxiliary heater, a MED desalination unit, and ETCs. The second one is based on LFRs, a MED desalination unit, a biomass auxiliary heater, and a double- effect ACH unit. Both systems are able to provide space heating and cooling, DHW, and freshwater. In their approach, the proposed polygeneration plants are simulated via a zero-dimensional dynamic model in TRNSYS environment. Their results demonstrate that, when MED is assisted by the biomass heater, the solar fraction for freshwater production varies from 15% to 20% for the ETC-based system in some winter weeks, while there is no

variation for the LFR-based system. As a result, their economic results reveal that ETCs are more profitable than LRFs with payback periods of 4 to 5 years.

Ghorbani et al. [84] have proposed an integrated structure for bio-liquefied natural gas (bio-LNG), freshwater, heating, and power production. Their solar-geothermal based system is composed of an upgraded biogas system, MED desalination, solar PV panels, and ORC. Their results show that the outputs of the hybrid system are 5.295 kg/s of bio-LNG, 2.773 kg/s of freshwater, and 840 kW of power. Their results also establish that the overall system energy and exergy efficiencies are 73.22% and 76.84%, respectively. Still, the exergy analysis indicates that the solar PV system has the highest rate of exergy destruction of 70.05%. Therefore, their study successfully demonstrates how the excess heat from the integrated system can be used to drive both the MED desalination and power generation in the ORC unit.

Ghorbani et al. [85] have performed a combined energy, exergy and economic evaluation of an integrated system composed of a cryogenic air separation unit, a ORC unit, a LNG regasification unit, oxy-fuel power plant, and a MED desalination unit. Their results reveal a thermal energy efficiency of 74.19% and an exergy efficiency of 91.73% for the integrated system under consideration. Their economic analysis also shows a prime cost of product equal to ~0.15 US$/kWh, a net benefit of 738.3 MMUS$ per year, and an investment return period of around 3.2 years. Therefore, the use of energy from hot output gas streams to operate both the MED desalination and power generation in the ORC unit can also present economic benefits. Table 2 presents the summary of topical research on renewable energy-driven polygeneration systems based on MED desalination.

**Table 2.** Summary of topical research on integrated renewable energy-driven polygeneration and MED desalination systems.

| Reference | Methodology | Products | Renewable Energy Source | Main Observations |
|---|---|---|---|---|
| Abdelhay et al. [80] | Thermodynamic, exergy, and economic analysis | Power, freshwater, and cooling | Solar PTC | - Integrated SPS, MED, and ARS<br>- Increasing MED number of effects<br>- Lower steam temperature increases GOR and PTC area |
| Calise et al. [81] | Thermodynamic and exergy optimization | Heat, cooling, and freshwater | Biomass and solar | - Transient simulation of a polygeneration plant based on evacuated tube collectors<br>- MED unit is driven by solar and biomass energy<br>- Best economic scenario is determined by Design of Experiment (DoE) optimization method |
| Vazini and Khoshgoftar Manesh [82] | Thermodynamic, exergy, economic, exergoeconomic, exergoenvironmental optimization | Power, freshwater, and cooling | Solar PTC | - Combined GT-absorption chiller-solar PTC-MED-TVC-RO system<br>- Optimization based on MOGA and MOWCA algorithms<br>- Results show an increase of 12.66% in exergy efficiency<br>- The total cost and environmental impact rate of the system decreased by 47.4$/h and 49.2 pts/h, respectively |
| Calise et al. [83] | Thermodynamic and economic analysis | Space heating and cooling, DHW, and freshwater | Solar and biomass | - Dynamic simulation<br>- Evaluation of the linear Fresnel and evacuated solar collectors integrated with thermal-driven desalination technologies<br>- Payback period of 4 to 5 years |

**Table 2.** *Cont.*

| Reference | Methodology | Products | Renewable Energy Source | Main Observations |
|---|---|---|---|---|
| Ghorbani et al. [84] | Thermodynamic, exergy, and exergoeconomic analysis | Bio-liquefied natural gas, desalted water, and power | Solar, biomass and geothermal | - Combined bio-LNG system, MED and ORC<br>- PV and geothermal energy are used to satisfy power and heating demands<br>- The hybrid system generates<br>- 5.295 kg/s of bio-LNG, 2.773 kg/s of desalted water, and 840 kW of power<br>- The power consumption of the liquefaction cycle is 0.1808 kWh/kg LNG<br>- Overall energy efficiency of 73.22%<br>- Overall exergy efficiency of 76.84% |
| Vazini and Khoshgoftar Manesh [86] | Thermodynamic, exergy, economic, exergoeconomic, exergoenvironmental and dynamic analysis | Power, freshwater, and cooling | Solar PTC | - 4E Dynamic analysis of a water-power cogeneration plant, combined with solar PTC and ACH<br>- Accurate thermodynamic analysis of MED-TVC<br>- PTC is used for feedwater preheating<br>- Dynamic simulation of ACH for inlet air cooling of the compressor |

Abbreviations: ACH, absorption chiller; ARS, Absorption Refrigeration System; GOR, gained output ratio; LNG, liquefied natural gas; MED, multi-effect distillation; MOGA, multi-objective genetic algorithm; MOWCA, multi-objective water cycle algorithm; ORC, organic Rankine cycle; PTC, parabolic trough collectors; RO, reverse osmosis; STS, solar thermal system; TVC, thermal vapor compressor.

### *5.3. Integrated Polygeneration and HDH Desalination Systems*

Some researchers have focused on integrating polygeneration and HDH desalination systems to improve the plant performance, whilst delivering several outputs such as power, space heating and cooling, and freshwater, to list but a few. In this way, Sahoo et al. [87] have developed a hybrid solar-biomass polygeneration system aimed at generating multiple outputs including power, space cooling, and freshwater. Thus, the proposed system is composed of a multi-effect HDH desalination unit for freshwater production, hybrid solar-biomass power plant for electricity production, and vapor absorption refrigeration for cooling generation. The authors have performed a thermodynamic evaluation and process optimization to identify the effects of different operating parameters on the polygeneration system performance. Figure 10 depicts the schematic diagram of the hybrid solar-biomass power plant with cooling and multi-effect HDH desalination as proposed by the authors. Their results show that the electricity generation from polygeneration system increases to 78.12%, when compared to the simple power plant operation. In addition, the primary energy savings are 50.5% for the polygeneration system, while the overall exergy efficiency is increased to 20.94% in comparison to the base case (i.e., simple power plant operation). Therefore, their renewable energy-driven polygeneration system constitutes a viable solution for decentralized applications.

Ghaebi et al. [88] have assessed the performance and optimization of an innovative renewable energy-driven polygeneration and desalination system in terms of thermodynamic and thermo-economic aspects. Their polygeneration system based on a geothermal heat source is used for the simultaneous production of cooling, heating, power, and freshwater. The authors have considered the integration of an absorption refrigeration cycle, a HDH desalination system, a Kalina power cycle, and domestic water heater unit. Their optimal results present overall system energy efficiency of 94.84%, overall exergy efficiency of 94.84%, and total unit cost of product of 89.95$/GJ. Rostamzadeh et al. [89] have proposed a polygeneration system powered by a hybrid biogas-geothermal heat source. The authors have performed an economic and environmental evaluation of the proposed biogas-geothermal polygeneration system. Moreover, they have developed single and multi-criteria optimization approaches to enhance the overall system performance. The

obtained results reveal that the total cost of the products can be decreased by 3.7% through optimization, whereas the thermal and exergy efficiencies are improved by 12.07% and 5.16%, respectively. Finally, their study includes a comprehensive sensitivity analysis based on the key economic system parameters. Therefore, this study highlights the benefits of combined polygeneration and desalination systems for areas with great availability of both biogas and low-temperature geothermal heat.

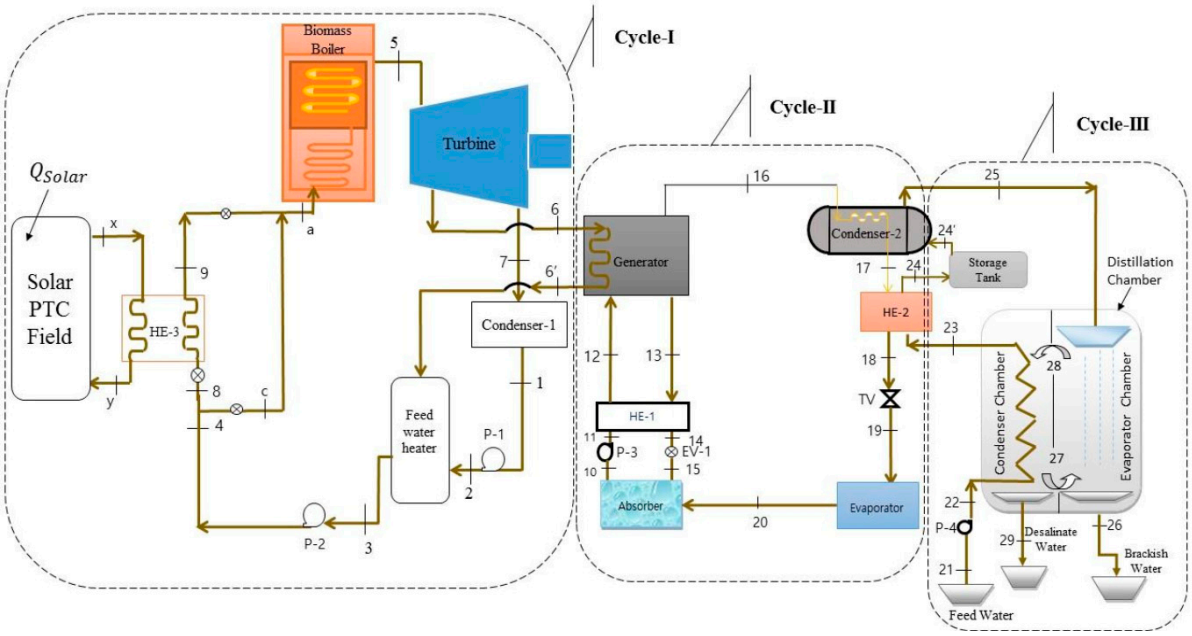


**Figure 10.** Schematic diagram of the hybrid solar-biomass power plant with cooling and multi-effect humidification-dehumidification (HDH) desalination proposed by Sahoo et al. [87].

Abbasti et al. [90] have proposed a multi-criteria optimization approach for enhancing a renewable energy-driven polygeneration system. Their proposed plant includes a hydrogen-based system, HDH desalination unit, and a thermoelectric generator. Hence, a proton exchange membrane electrolyzer (PEME) is used to produce hydrogen, whereas the HDH is applied for freshwater production. In their proposed polygeneration system, a Kalina power cycle and a thermoelectric generator (TEG) are used to provide the electricity required by the PEME system. The authors have performed an exergoeconomic analysis to evaluate the recommended configurations. Their results indicate an overall exergy efficiency for the optimal system configuration of 22.49%.

Li et al. [91] have simulated dynamically a solar-assisted polygeneration system for producing heat, power, and freshwater. Thus, their system integrates a solar thermal power (STP) tower plant, an absorption heat pump (AHP), and HDH desalination for freshwater production. Their results show that the proposed variable operation modes are suitable for flexible heating loads ranging from 93.76 to 169.49 kW. Still, the coefficient of performance (COP) in the AHP operation presents a range of 1.39 to 1.73 due to the restriction of recoverable condensate heat by heating demand. Their results also reveal that the generation of freshwater by the HDH desalination unit increased from 352.05 kg/h to 416.62 kg/h, with a corresponding elevation in the gained output ratio (GOR) from 2.48 to 2.67. Moreover, the maximum power production efficiency is increased from 18.66% to 19.22%, while power production raises from 1169.69 to 1204.44 kW when compared to the STP tower plant. Table 3 presents the summary of topical research on renewable energy-driven polygeneration systems based on HDH desalination.

**Table 3.** Summary of topical research on integrated renewable energy-driven polygeneration and HDH desalination systems.

| Reference | Methodology | Products | Renewable Energy Source | Main Observations |
|---|---|---|---|---|
| Sahoo et al. [87] | Thermodynamic and exergy analysis | Power, cooling, and freshwater | Solar PTC and biomass | - Analysis of combined Rankine cycle, VAR and CAOW-WH-HDH<br>- LiBr-$H_2O$ is used as refrigerant<br>- Application of biomass with solar energy to deal with periodicity of solar energy<br>- Heat from turbine applied for VAR cooling and desalination<br>- Maximum energy efficiency of 49.35%<br>- Maximum exergy efficiency of 20.47% |
| Ghaebi et al. [88] | Thermodynamic, exergy, economic, and exergoeconomic analysis | Heating, cooling, and freshwater | Geothermal | - Integrated Kalina, VAR, Heating, and CAOW-WH HDH multi-system<br>- Multi-objective optimization applied to maximize the energy and exergy efficiencies, and minimize the total cost<br>- The system produces 3010 kW of electricity, kW of cooling, 9527 kW of heating, and 8.923 kg/s of freshwater<br>- Optimal thermal efficiency of 94.84%<br>- Optimal exergy efficiency is 47.89% |
| Rostamzadeh et al. [89] | Thermodynamic, economic, and environmental optimization | Heating, cooling, power, hydrogen, and freshwater | Biogas and geothermal | - Combined Kalina, VAR, Heating, Hydrogen, and CAOW-WH system<br>- The system produces 538.1 kW of heating, 1799 kW of cooling, 443.4 kW of power, 0.2586 kg/s of hydrogen, and 367.92 l/h freshwater<br>- The optimization improves thermal and exergy efficiencies improved by 12.07% and 5.16%, respectively |
| Abbasi et al. [90] | Thermodynamic, economic, exergy, and exergoeconomic multi-objective optimization | Freshwater and hydrogen | Geothermal | - Two cogeneration systems are presented to the integration of PEME and HDH units, Kalina cycle, and TEG<br>- In the optimal design, the total exergy efficiency is 22.49% |
| Li et al. [91] | Thermodynamic dynamic analysis | Heating, power, and freshwater | Solar | - Transient simulation of a solar polygeneration system based on STP tower plant<br>- A case study is investigated based on 1 MW STP plant in Beijing<br>- Integrated solar-driven AHP and HDH system is compared to the base plant<br>- The maximum electricity generation efficiency is increased from 18.66% to 19.22% |

Abbreviations: AHP, absorption heat pump; CAOW, closed-air open-water; HDH, humidification-dehumidification; PEME, proton exchange membrane electrolyzer; STP, solar thermal power; TEG, thermoelectric generator; VAR, vapor absorption refrigeration; WH, water-heated.

### *5.4. Integrated Polygeneration and RO Desalination Systems*

El-Emam and Dincer [92] have comprehensively analyzed the thermodynamics of an integrated solar-based polygeneration system using energy and exergy approaches. Their recommended system is based on a heliostat solar system combined with a steam turbine. Furthermore, the authors have considered a seawater RO desalination unit coupled to an ACS unit. The desalination unit operates with energy recovery by utilizing a Pelton turbine. Cooling, heating, freshwater, and hydrogen are outputs of the proposed system. Their results show that the polygeneration system can meet the electric power demand of 4 MW, and provide additional 1.25 kg/h of hydrogen and 90 kg/s of freshwater. Another solar-based polygeneration system consisting of a RO desalination unit, water heater,

ORC, PV solar collectors, and a single-effect ACH have been analyzed by Rashidi and Khorshidi [93]. First, the authors have performed an energy and exergy analysis of the integrated system. Then, they have developed a multi-objective optimization approach based on a differential evolution algorithm for obtaining the optimal design parameters. In this regard, the minimization of total process cost, and maximization of exergy efficiency have been considered as the objective functions. Still, the authors have applied a fuzzy clustering approach for selecting the most favorable solution out of the Pareto-optimal ones. Their simulation results have been compared with two other multi-objective optimization algorithms. The authors have also carried out a sensitivity analysis to examine the impacts of design parameters on system exergy efficiency and total cost rate.

Islam et al. [94] have performed a comparative energy and exergy analysis of an integrated polygeneration system based on solar energy and two different configurations of thermoelectric generators. Their first system layout integrates the output of the thermoelectric generator with the parabolic solar collectors, while the second one incorporates the thermoelectric generators between the ORC and solar heat exchanger. The authors have assessed the effects of the distinct design configurations and operating conditions on the overall energy and exergy efficiencies of the polygeneration system. Their findings suggest that the work rate of turbines and thermoelectric generators can be improved by increasing the mass flowrate of the solar heat fluid. In addition, the proposed systems are better than the corresponding conventional ones in terms of thermoelectric generation.

Mouaky and Rachek [95] have evaluated a polygeneration system combining a solar compound parabolic collectors (CPCs) field, a thermocline TES unit, biomass-fired boilers, an ORC unit, a RO desalination unit, a hybrid air/water condenser, and a vapor compression cycle. The authors have examined the energy, exergy, and exergoeconomic indicators of the polygeneration system. Still, they have considered a community of 40 households located at a semi-arid region in Benguerir, Morocco, which is characterized by great solar potential and brackish groundwater. Their results indicate that the polygeneration system can be a suitable solution for the region, due to its ability to fulfill several demands at once. Their system presents an annual biomass consumption of 342 T with an average solar contribution of 20% (i.e., 20% of the total energy required by the ORC unit is provided by the solar field). Moreover, the overall energy efficiency of the polygeneration system ranges between 15% to 44%, while the corresponding exergy efficiency varies from 5% to 2.9%. Finally, the parametric economic evaluation carried out by the authors demonstrates that considerable decreases in the cost of the solar field should be achieved to make the aperture elevate economically viable.

Tan et al. [96] have studied the integration of RO desalination and indirect ocean capture system to reduce carbon emissions. Their polygeneration system combines cooling, heating, hydrogen chloride (HCl), $CO_2$-absorbing brine, freshwater, and power generation. The authors have developed a mixed-integer linear programming (MILP) model for the optimal synthesis and operation of this type of system. Their model takes advantage of multi-period formulation to account for the variations in product demands and electricity prices in different time periods. They have also carried out a sensitivity analysis to study the parametric system uncertainties. Their results reveal that the operation of the electrolysis unit along with the demand for HCl storage depend on the electricity grid carbon footprint.

Siddiqui and Dincer [97] have developed an integrated polygeneration system based on solar and geothermal energy for producing electricity, hydrogen, cooling, and freshwater. Moreover, their system encompasses a cell subsystem with solar integrated ammonia fuel, and a hydrogen generation system based on a proton exchange membrane. A RO desalination unit is used to produce freshwater. In addition, an ACS is applied for district cooling by taking advantage of the existing waste heat of the system. The authors have presented a thermodynamic evaluation of the proposed system through energy and exergy analyses. Their results indicate overall energy and exergy efficiencies of 42.3% and 21.3%, respectively. The results also show that the cooling system generator and geothermal flash chamber have the highest rates of exergy destruction of 2370.2 kW and 643.3 kW, correspondingly.

A comparison between the performances of a natural gas and renewable-based polygeneration system have been presented by Al-Obaidli et al. [81]. In their study, the authors have considered a hybrid solar-biomass polygeneration plant composed of combined steam Rankine and gas Brayton cycles, a solar thermal cycle, an ACS, and a RO unit for desalination. Their results indicate that the proposed system presents only slightly higher efficiencies against the reference system (in which MSF substitutes the RO unit) on the basis of cogeneration. Yet, when considering polygeneration, the proposed alternative system presents increased overall energy and exergy efficiencies of 62.9% and 41.9%, respectively. Table 4 presents the summary of topical research on renewable energy-driven polygeneration systems based on RO desalination.

**Table 4.** Summary of topical research on integrated renewable energy-driven polygeneration and RO desalination systems.

| Reference | Methodology | Products | Renewable Energy Source | Main Observations |
|---|---|---|---|---|
| El-Emam and Dincer [92] | Thermodynamic and exergy analysis | Cooling, heating, freshwater, and hydrogen | Heliostat solar | - Development and assessment of a solar heliostat-based polygeneration system<br>- Production of 4 MW of electric power, 1.25 kg/h of hydrogen, and 90 kg/s of freshwater |
| Rashidi and Khorshidi [93] | Thermodynamic, exergy, and exergoeconomic optimization | Heating, cooling, power, and freshwater | PV solar | - Multi-objective differential evolution algorithm for system optimization |
| Islam et al. [94] | Thermodynamic and exergy analysis | Heating, cooling, power, freshwater, and hydrogen | Parabolic solar collectors | - Analysis and evaluation of PTC based system with thermoelectric generator<br>- Energy and exergy efficiencies of total system are improved<br>- The work output by ORC is also improved |
| Mouaky and Rachek [95] | Thermodynamic, exergy, and exergoeconomic analysis | Electricity, freshwater, DHW, space heating, and cooling | Solar and biomass | - Analysis of a hybrid solar-biomass polygeneration system<br>- A case study of a rural community in a semi-arid climate is performed<br>- Overall energy efficiency of 8.25%<br>- Overall exergy efficiency of 3.89%<br>- Employing R1336mzz(Z) instead of R245-fa could decreased the biomass consumption by 13.4% |
| Tan et al. [96] | Thermodynamic, exergy, and exergoeconomic analysis | Power, freshwater, steam, HCl and $CO_2$ | Biomass | - Optimal design of negative emissions polygeneration systems with desalination<br>- Desalination reject brine is treated to absorb and react with CO2 in air<br>- A multi-period MILP model is proposed for the optimal design of the system<br>- Sensitivity analysis regarding the capital cost and carbon tax is carried out |
| Siddiqui and Dincer [97] | Thermodynamic, exergy, and exergoeconomic analysis | Freshwater, hydrogen, and district cooling | Solar and geothermal | - A solar and geothermal based multigeneration system is combined with ammonia fuel cell<br>- Overall energy efficiency system of 42.3%<br>- Overall exergy efficiency of 21.3% |
| Al-Obaidli et al. [81] | Thermodynamic and exergy analysis | Power, freshwater, and district heating | Biomass and solar | - Performance evaluation of a natural gas and renewable energy-based desalination and power generation<br>- Energy efficiency of 62.9%<br>- Exergy efficiency of 41.9% |

Abbreviations: DHW, domestic hot water; MILP; mixed-integer linear programming; ORC, organic Rankine cycle; PTC, parabolic trough collectors; PV, photovoltaic; RO, reverse osmosis.

### *5.5. Other Integrated Polygeneration and Desalination Systems*

Ayou et al. [98] have developed a numerical modelling approach to investigate the energy and exergy performance of a renewable energy-driven polygeneration system. Their polygeneration system integrates an ammonia/water absorption power-refrigeration system driven by an evacuated flat plate solar collectors' field and a biomass-fired backup boiler, and a desalination system based on permeate/conductive-gap membrane distillation modules. Thus, the polygeneration system is designed to provide the energy needed for space cooling, electricity, and freshwater. Figure 11 displays the schematic diagram of the hybrid solar-biomass polygeneration system proposed by the authors. Ayou et al. [98] have evaluated the overall energy and exergy efficiencies of the a decentralized small-scale polygeneration plant by accounting for the weather conditions of a typical location in Spain, which presents high abundance of solar irradiation, high cooling demands, and great potential for freshwater shortages. Their results show that the system is able to produce up to 130 kW of cooling load capacity at 11 °C, 6.4 kW of net electrical power, and 41.4 $m^3$/day of freshwater depending on the average local weather conditions. In addition, the overall system exergy and resource utilization efficiencies are equal to 6.9% and 44.2%, respectively. Their results also reveal that the implementation of an integrated solar-biomass-driven absorption refrigeration system and membrane desalination system can increase the efficiency of the whole thermal energy conversion process. Furthermore, this may result in a cost-effective utilization of solar thermal installation, especially in areas where desalination is necessary.

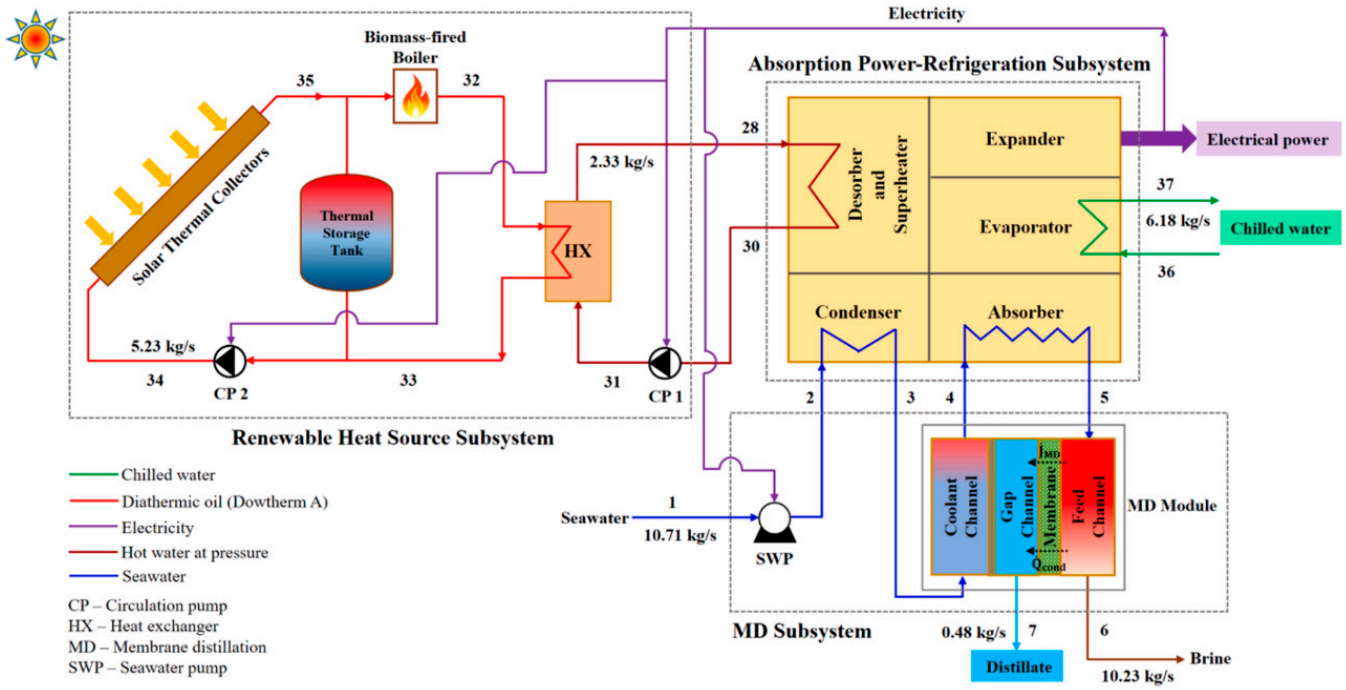


**Figure 11.** Schematic diagram of the hybrid solar-biomass polygeneration system, as proposed by Ayou et al. [98].

## 6. Conclusions

Sustainable production of both freshwater and energy is vital for the continuous development of modern societies. For this reason, considerable research has been carried out over the last few decades to investigate alternatives for addressing ever-increasing water and energy demands while protecting the environment. Integrated decentralized polygeneration and desalination systems have emerged as a suitable solution for remote areas, particularly when assisted by renewable energy sources. Within this framework, this review addresses the most recent developments in integrated renewable energy-driven

decentralized polygeneration systems considering thermal and membrane desalination. Thus, polygeneration systems coupled to MSF, MED, HDH, and RO desalination technologies are outlined as an effective and sustainable alternative for freshwater production, mainly in isolated locations and communities. In addition to freshwater production, polygeneration plants accounting for electricity, space heating and cooling, domestic hot water, among other useful outputs, are reviewed in this paper. Furthermore, different renewable energy resources are considered, such as solar, biomass, geothermal, ocean, wind, and hybrid renewable energy systems. Special attention is given to the most innovative approaches for modelling, design, simulation, and optimization of decentralized integrated polygeneration and desalination plants especially aimed at improving energy, exergy, and thermo-economic system performance.

The literature reviewed shows that comprehensive energy, exergy, and thermo-economic analyses are imperative for enhancing energy, exergy, and economic performance of integrated renewable energy-driven polygeneration and desalination systems. Still, advanced exergy-related approaches including exergoeconomic and exergoenvironmental analysis tools present great potential to more accurately appraise the corresponding system economic and environmental performances. Nevertheless, the pertaining literature is still quite limited regarding the development of multi-objective optimization approaches to simultaneously assess energy, exergy, economic, and environmental system performances. The application of multi-objective optimization methodologies would enable to evaluate trade-offs between different optimization objectives, whilst enhancing the system energy and/or exergy efficiency. In addition, more precise modelling and optimization approaches should be developed to account for distinct sources of uncertainty in polygeneration and desalination systems. Uncertain factors can include fluctuating scenarios of renewable energy production due to intermittency in weather conditions, biomass availability, variable energy and water demands throughout different time periods, to name but a few. Finally, further developments in integrated renewable energy-driven polygeneration and desalination system will certainly be driven by more appealing policies and stricter environmental impact regulations, together with technological advancements in energy conversion, efficiency, and storage.

**Author Contributions:** Conceptualization, V.C.O.; methodology, M.H.K.M.; formal analysis, M.H.K.M. and V.C.O.; investigation, M.H.K.M. and V.C.O.; resources, V.C.O.; data curation, M.H.K.M. and V.C.O.; writing—original draft preparation, M.H.K.M.; writing—review and editing, V.C.O.; visualization, V.C.O. All authors have read and agreed to the published version of the manuscript.

**Funding:** This research received no external funding.

**Institutional Review Board Statement:** Not applicable.

**Informed Consent Statement:** Not applicable.

**Data Availability Statement:** Not applicable.

**Conflicts of Interest:** The authors declare no conflict of interest.

## Nomenclature

Acronyms

| | |
|---|---|
| ACH | Absorption chiller |
| ACS | Absorption cooling system |
| AD | Adsorption desalination |
| AH-HDH | Air-heated humidification-dehumidification |
| AHP | Absorption heat pump |
| ARS | Absorption refrigeration system |
| BR | Brine recirculation |
| BWD | Brackish water desalination |
| CAOW | Closed-air open-water |
| COP | Coefficient of performance |

| | |
|---|---|
| CPC | Compound parabolic collector |
| CPV | Concentrated photovoltaic |
| CPVT | Concentrated photovoltaic thermal |
| CSP | Concentrated solar power |
| DHW | Domestic hot water |
| DoE | Design of Experiment |
| DSG | Direct steam generator |
| ETC | Evacuated tube solar collectors |
| EWF | Energy-water-food nexus |
| GOR | Gained output ratio |
| HCl | Hydrogen chloride |
| HDH | Humidification-dehumidification |
| IEA | International Energy Agency |
| LFR | Linear Fresnel reflectorxxxx |
| LNG | Liquefied natural gas |
| MED | Multi-effect distillation |
| MILP | Mixed-integer linear programming |
| MOGA | Multi-objective genetic algorithm |
| MOWCA | Multi-objective water cycle algorithm |
| MSF | Multi-stage flash |
| MVC | Mechanical vapor compression |
| NG-CS | Natural gas-compressor station |
| OACW | Open-air closed-water |
| OAOW | Open-air open-water |
| ORC | Organic Rankine cycle |
| OT | Once through |
| OTEC | Ocean thermal energy conversion |
| PEME | Proton exchange membrane electrolyzer |
| PRO | Pressure retarded osmosis |
| PTC | Parabolic trough collectors |
| PV | Photovoltaic |
| PVT | Photovoltaic thermal |
| RO | Reverse osmosis |
| STP | Solar thermal power |
| SWD | Seawater desalination |
| TEG | Thermoelectric generator |
| TBT | Top brine temperature |
| TES | Thermal energy storage |
| TTD | Total temperature difference |
| TVC | Thermal vapor compression |
| VAR | Vapor absorption refrigeration |
| VCR | Vapor compression refrigeration |
| WH | Waste heat |
| WH-HDH | Water-heated humidification-dehumidification |

## References

1. IEA; International Renewable Energy Agency; United Nations Statistics Division; The World Bank. *World Health Organization The Energy Progress Report*; IREA: Abu Dhabi, UAE, 2019; p. 176.
2. IEA; IRENA; UNSD; World Bank. *WHO Tracking SDG 7: The Energy Progress Report*; World Bank: Washington, DC, USA, 2020; p. 176.
3. Mouaky, A.; Rachek, A. Thermodynamic and thermo-economic assessment of a hybrid solar/biomass polygeneration system under the semi-arid climate conditions. *Renew. Energy* **2020**, *156*, 14–30. [CrossRef]
4. Alstone, P.; Gershenson, D.; Kammen, D.M. Decentralized energy systems for clean electricity access. *Nat. Clim. Chang.* **2015**, *5*, 305–314. [CrossRef]

5. Jana, K.; Ray, A.; Majoumerd, M.M.; Assadi, M.; De, S. Polygeneration as a future sustainable energy solution—A comprehensive review. *Appl. Energy* **2017**, *202*, 88–111. [CrossRef]
6. United Nations. *The Sustainable Development Goals Report 2020*; United Nations: New York, NY, USA, 2020.
7. United Nations. *The Sustainable Development Goals Report 2019*; United Nations: New York, NY, USA, 2019; p. 64.
8. Boretti, A.; Rosa, L. Reassessing the projections of the World Water Development Report. *NPJ Clean Water* **2019**, *2*, 1–6. [CrossRef]
9. Lattemann, S.; Kennedy, M.D.; Schippers, J.C.; Amy, G. Chapter 2 Global Desalination Situation. In *Sustainable Water for the Future: Water Recycling Versus Desalination*; Escobar, I.C., Schäfer, A., Eds.; Elsevier: Amsterdam, The Netherlands, 2010; Volume 2, pp. 7–39, ISBN 1871-2711.
10. Ghaffour, N.; Missimer, T.M.; Amy, G.L. Technical review and evaluation of the economics of water desalination: Current and future challenges for better water supply sustainability. *Desalination* **2013**, *309*, 197–207. [CrossRef]
11. Schallenberg-Rodríguez, J.; Veza, J.M.; Blanco-Marigorta, A. Energy efficiency and desalination in the Canary Islands. *Renew. Sustain. Energy Rev.* **2014**, *40*, 741–748. [CrossRef]
12. Mohammadi, K.; Khaledi, M.S.E.; Saghafifar, M.; Powell, K. Hybrid systems based on gas turbine combined cycle for trigeneration of power, cooling, and freshwater: A comparative techno-economic assessment. *Sustain. Energy Technol. Assess.* **2020**, *37*, 100632. [CrossRef]
13. Shahzad, M.W.; Burhan, M.; Ng, K.C. A standard primary energy approach for comparing desalination processes. *NPJ Clean Water* **2019**, *2*, 1–7. [CrossRef]
14. Jones, E.; Qadir, M.; van Vliet, M.T.H.; Smakhtin, V.; Kang, S. The state of desalination and brine production: A global outlook. *Sci. Total Environ.* **2019**, *657*, 1343–1356. [CrossRef]
15. Fritzmann, C.; Löwenberg, J.; Wintgens, T.; Melin, T. State-of-the-art of reverse osmosis desalination. *Desalination* **2007**, *216*, 1–76. [CrossRef]
16. Salcedo, R.; Antipova, E.; Boer, D.; Jiménez, L.; Guillén-Gosálbez, G. Multi-objective optimization of solar Rankine cycles coupled with reverse osmosis desalination considering economic and life cycle environmental concerns. *Desalination* **2012**, *286*, 358–371. [CrossRef]
17. Al-Karaghouli, A.; Kazmerski, L.L. Energy consumption and water production cost of conventional and renewable-energy-powered desalination processes. *Renew. Sustain. Energy Rev.* **2013**, *24*, 343–356. [CrossRef]
18. Semiat, R.; Hasson, D. Water desalination. *Rev. Chem. Eng.* **2012**, *28*, 43–60. [CrossRef]
19. Olabi, A.G.; Elsaid, K.; Rabaia, M.K.H.; Askalany, A.A.; Abdelkareem, M.A. Waste heat-driven desalination systems: Perspective. *Energy* **2020**, *209*, 118373. [CrossRef]
20. Lattemann, S.; Höpner, T. Environmental impact and impact assessment of seawater desalination. *Desalination* **2008**, *220*, 1–15. [CrossRef]
21. Gude, V.G. Energy storage for desalination processes powered by renewable energy and waste heat sources. *Appl. Energy* **2015**, *137*, 877–898. [CrossRef]
22. Mahmoudi, A.; Fazli, M.; Morad, M.R. A recent review of waste heat recovery by Organic Rankine Cycle. *Appl. Therm. Eng.* **2018**, *143*, 660–675. [CrossRef]
23. Zhang, X.; Liu, Y.; Wen, X.; Li, C.; Hu, X. Low-grade waste heat driven desalination with an open loop heat pipe. *Energy* **2018**, *163*, 221–228. [CrossRef]
24. Jouhara, H.; Khordehgah, N.; Almahmoud, S.; Delpech, B.; Chauhan, A.; Tassou, S.A. Waste heat recovery technologies and applications. *Therm. Sci. Eng. Prog.* **2018**, *6*, 268–289. [CrossRef]
25. Tavakkoli, S.; Lokare, O.R.; Vidic, R.D.; Khanna, V. Systems-level analysis of waste heat recovery opportunities from natural gas compressor stations in the United States. *ACS Sustain. Chem. Eng.* **2016**, *4*, 3618–3626. [CrossRef]
26. Lokare, O.R.; Tavakkoli, S.; Rodriguez, G.; Khanna, V.; Vidic, R.D. Integrating membrane distillation with waste heat from natural gas compressor stations for produced water treatment in Pennsylvania. *Desalination* **2017**, *413*, 144–153.
27. Saari, R. Usability of low temperature waste heat for sea water desalination. *Desalination* **1981**, *39*, 147–158. [CrossRef]
28. Abdelkareem, M.A.; El Haj Assad, M.; Sayed, E.T.; Soudan, B. Recent progress in the use of renewable energy sources to power water desalination plants. *Desalination* **2018**, *435*, 97–113.
29. Rezk, H.; Sayed, E.T.; Al-Dhaifallah, M.; Obaid, M.; El-Sayed, A.H.M.; Abdelkareem, M.A.; Olabi, A.G. Fuel cell as an effective energy storage in reverse osmosis desalination plant powered by photovoltaic system. *Energy* **2019**, *175*, 423–433. [CrossRef]
30. Alvarado-Revilla, F. *Desalination Markets 2016: Global Perspective and Opportunities for Growth*; Media Analytics Limited: Oxford, UK, 2015.
31. Khawaji, A.D.; Kutubkhanah, I.K.; Wie, J.M. Advances in seawater desalination technologies. *Desalination* **2008**, *221*, 47–69.
32. Tusel, G.F.; Rautenbach, R.; Widua, J. Seawater desalination plant "Sirte"—An example for an advanced MSF design. *Desalination* **1994**, *96*, 379–396. [CrossRef]
33. Mabrouk, A.N.A. Technoeconomic analysis of once through long tube MSF process for high capacity desalination plants. *Desalination* **2013**, *317*, 84–94. [CrossRef]
34. Hamed, O.A.; Al-Sofi, M.A.K.; Imam, M.; Mustafa, G.M.; Ba Mardouf, K.; Al-Washmi, H. Thermal performance of multi-stage flash distillation plants in Saudi Arabia. *Desalination* **2000**, *128*, 281–292. [CrossRef]
35. Voutchkov, N. *Desalination Engineering: Planning and Design*; McGraw Hill Professional: New York, NY, USA, 2012; ISBN 0071777164.

36. Mezher, T.; Fath, H.; Abbas, Z.; Khaled, A. Techno-economic assessment and environmental impacts of desalination technologies. *Desalination* **2011**, *266*, 263–273. [CrossRef]
37. Alhazmy, M.M. Economic and thermal feasibility of multi stage flash desalination plant with brine–feed mixing and cooling. *Energy* **2014**, *76*, 1029–1035. [CrossRef]
38. Hanshik, C.; Jeong, H.; Jeong, K.-W.; Choi, S.-H. Improved productivity of the MSF (multi-stage flashing) desalination plant by increasing the TBT (top brine temperature). *Energy* **2016**, *107*, 683–692. [CrossRef]
39. El-Dessouky, H.T.; Ettouney, H.M. *Fundamentals of Salt Water Desalination*; Elsevier: Amsterdam, The Netherlands, 2002; ISBN 0080532128.
40. Water, U.N. Policy Brief: Water Quality. United Nations. 2011. Available online: http//www.unwater.org/downloads/waterquality_policybrief.pdf (accessed on 20 December 2020).
41. Hawaidi, E.A.M.; Mujtaba, I.M. Simulation and optimization of MSF desalination process for fixed freshwater demand: Impact of brine heater fouling. *Chem. Eng. J.* **2010**, *165*, 545–553. [CrossRef]
42. Al-Hamahmy, M.; Fath, H.E.S.; Khanafer, K. Techno-economical simulation and study of a novel MSF desalination process. *Desalination* **2016**, *386*, 1–12. [CrossRef]
43. Bazargan, A. *A Multidisciplinary Introduction to Desalination*; Stylus Publishing, LLC: Sterling, VA, USA, 2018; ISBN 8793609949.
44. Al-Shammiri, M.; Safar, M. Multi-effect distillation plants: State of the art. *Desalination* **1999**, *126*, 45–59. [CrossRef]
45. Raluy, G.; Serra, L.; Uche, J. Life cycle assessment of MSF, MED and RO desalination technologies. *Energy* **2006**, *31*, 2361–2372. [CrossRef]
46. Nassrullah, H.; Anis, S.F.; Hashaikeh, R.; Hilal, N. Energy for desalination: A state-of-the-art review. *Desalination* **2020**, *491*, 114569. [CrossRef]
47. Darwish, M.A.; Alsairafi, A. Technical comparison between TVC/MEB and MSF. *Desalination* **2004**, *170*, 223–239. [CrossRef]
48. Al-Mutaz, I.S.; Wazeer, I. Development of a steady-state mathematical model for MEE-TVC desalination plants. *Desalination* **2014**, *351*, 9–18. [CrossRef]
49. Morin, O.J. Design and operating comparison of MSF and MED systems. *Desalination* **1993**, *93*, 69–109. [CrossRef]
50. Milow, B.; Zarza, E. Advanced MED solar desalination plants. Configurations, costs, future—seven years of experience at the Plataforma Solar de Almeria (Spain). *Desalination* **1997**, *108*, 51–58. [CrossRef]
51. Nair, M.; Kumar, D. Water desalination and challenges: The Middle East perspective: A review. *Desalin. Water Treat.* **2013**, *51*, 2030–2040. [CrossRef]
52. Saldivia, D.; Rosales, C.; Barraza, R.; Cornejo, L. Computational analysis for a multi-effect distillation (MED) plant driven by solar energy in Chile. *Renew. Energy* **2019**, *132*, 206–220. [CrossRef]
53. Al-Mutaz, I.S.; Wazeer, I. Optimization of location of thermo-compressor suction in MED-TVC desalination plants. *Desalin. Water Treat.* **2016**, *57*, 26562–26576. [CrossRef]
54. Fiorenza, G.; Sharma, V.K.; Braccio, G. Techno-economic evaluation of a solar powered water desalination plant. *Energy Convers. Manag.* **2003**, *44*, 2217–2240. [CrossRef]
55. Mayor, B. Growth patterns in mature desalination technologies and analogies with the energy field. *Desalination* **2019**, *457*, 75–84. [CrossRef]
56. Faegh, M.; Behnam, P.; Shafii, M.B. A review on recent advances in humidification-dehumidification (HDH) desalination systems integrated with refrigeration, power and desalination technologies. *Energy Convers. Manag.* **2019**, *196*, 1002–1036. [CrossRef]
57. He, W.F.; Wu, F.; Wen, T.; Kong, Y.P.; Han, D. Cost analysis of a humidification dehumidification desalination system with a packed bed dehumidifier. *Energy Convers. Manag.* **2018**, *171*, 452–460. [CrossRef]
58. Dehghani, S.; Date, A.; Akbarzadeh, A. An experimental study of brine recirculation in humidification-dehumidification desalination of seawater. *Case Stud. Therm. Eng.* **2019**, *14*, 100463. [CrossRef]
59. Xu, H.; Sun, X.Y.; Dai, Y.J. Thermodynamic study on an enhanced humidification-dehumidification solar desalination system with weakly compressed air and internal heat recovery. *Energy Convers. Manag.* **2019**, *181*, 68–79. [CrossRef]
60. Greenlee, L.F.; Lawler, D.F.; Freeman, B.D.; Marrot, B.; Moulin, P. Reverse osmosis desalination: Water sources, technology, and today's challenges. *Water Res.* **2009**, *43*, 2317–2348. [CrossRef]
61. Amidpour, M.; Khoshgoftar Manesh, M.H. Chapter 8-Desalinated water production in cogeneration and polygeneration systems. In *Cogeneration and Polygeneration Systems*; Amidpour, M., Khoshgoftar Manesh, M.H., Eds.; Academic Press: Cambridge, MA, USA, 2021; pp. 115–135, ISBN 978-0-12-817249-0.
62. Sharon, H.; Reddy, K.S. A review of solar energy driven desalination technologies. *Renew. Sustain. Energy Rev.* **2015**, *41*, 1080–1118. [CrossRef]
63. Blanco-Marigorta, A.M.; Lozano-Medina, A.; Marcos, J.D. A critical review of definitions for exergetic efficiency in reverse osmosis desalination plants. *Energy* **2017**, *137*, 752–760. [CrossRef]
64. Amidpour, M.; Khoshgoftar Manesh, M.H. Chapter 13-Modern polygeneration systems. In *Cogeneration and Polygeneration Systems*; Amidpour, M., Khoshgoftar Manesh, M.H., Eds.; Academic Press: Cambridge, MA, USA, 2021; pp. 237–286, ISBN 978-0-12-817249-0.
65. Wenzel, H. Biofuels: The good, the bad, the ugly—and the unwise policy. *Clean Technol. Environ. Policy* **2009**, *11*, 143–145. [CrossRef]

66. Ranjan, K.R.; Kaushik, S.C. Energy, exergy and thermo-economic analysis of solar distillation systems: A review. *Renew. Sustain. Energy Rev.* **2013**, *27*, 709–723. [CrossRef]
67. Li, Z.; Khanmohammadi, S.; Khanmohammadi, S.; Al-Rashed, A.A.A.A.; Ahmadi, P.; Afrand, M. 3-E analysis and optimization of an organic rankine flash cycle integrated with a PEM fuel cell and geothermal energy. *Int. J. Hydrogen Energy* **2019**, *45*, 2168–2185. [CrossRef]
68. Janghorban Esfahani, I.; Lee, S.C.; Yoo, C.K. Evaluation and optimization of a multi-effect evaporation-absorption heat pump desalination based conventional and advanced exergy and exergoeconomic analyses. *Desalination* **2015**, *359*, 92–107. [CrossRef]
69. Calise, F.; Dentice d'Accadia, M.; Piacentino, A.; Vicidomini, M. Thermoeconomic optimization of a renewable polygeneration system serving a small isolated community. *Energies* **2015**, *8*, 995–1024. [CrossRef]
70. Dincer, I.; Rosen, M.A. *Exergy: Energy, Environment and Sustainable Development*; Newnes: Oxford, UK, 2012; ISBN 0080970907.
71. Al-Weshahi, M.A.; Anderson, A.; Tian, G. Exergy efficiency enhancement of MSF desalination by heat recovery from hot distillate water stages. *Appl. Therm. Eng.* **2013**, *53*, 226–233. [CrossRef]
72. Sharqawy, M.H.; Lienhard, V.J.H.; Zubair, S.M. On exergy calculations of seawater with applications in desalination systems. *Int. J. Therm. Sci.* **2011**, *50*, 187–196. [CrossRef]
73. Calise, F.; Macaluso, A.; Piacentino, A.; Vanoli, L. A novel hybrid polygeneration system supplying energy and desalinated water by renewable sources in Pantelleria Island. *Energy* **2017**, *137*, 1086–1106. [CrossRef]
74. Hogerwaard, J.; Dincer, I.; Naterer, G.F. Solar energy based integrated system for power generation, refrigeration and desalination. *Appl. Therm. Eng.* **2017**, *121*, 1059–1069. [CrossRef]
75. Azhar, M.S.; Rizvi, G.; Dincer, I. Integration of renewable energy based multigeneration system with desalination. *Desalination* **2017**, *404*, 72–78. [CrossRef]
76. Sezer, N.; Koç, M. Development and performance assessment of a new integrated solar, wind, and osmotic power system for multigeneration, based on thermodynamic principles. *Energy Convers. Manag.* **2019**, *188*, 94–111.
77. Luqman, M.; Bicer, Y.; Al-Ansari, T. Thermodynamic analysis of an oxy-hydrogen combustor supported solar and wind energy-based sustainable polygeneration system for remote locations. *Int. J. Hydrogen Energy* **2020**, *45*, 3470–3483. [CrossRef]
78. Luqman, M.; Ghiat, I.; Maroof, M.; Lahlou, F.; Bicer, Y.; Al-Ansari, T. Application of the concept of a renewable energy based-polygeneration system for sustainable thermal desalination process—A thermodynamics' perspective. *Int. J. Energy Res.* **2020**, *44*, 12344–12362. [CrossRef]
79. Luqman, M.; Al-Ansari, T. Thermodynamic analysis of an Energy-Water-Food (Ewf) nexus driven polygeneration system applied to coastal communities. *Energy Convers. Manag.* **2020**, *205*, 112432.
80. Abdelhay, A.; Fath, H.S.; Nada, S.A. Solar driven polygeneration system for power, desalination and cooling. *Energy* **2020**, *198*, 117341.
81. Al-Obaidli, H.; Bicer, Y.; Al-Ansari, T. Performance comparison of a natural gas and renewable-based power and desalination system for polygeneration. *Greenh. Gases Sci. Technol.* **2020**, *10*, 678–702. [CrossRef]
82. Vazini Modabber, H.; Khoshgoftar Manesh, M.H. Optimal exergetic, exergoeconomic and exergoenvironmental design of polygeneration system based on gas Turbine-Absorption Chiller-Solar parabolic trough collector units integrated with multi-effect desalination-thermal vapor compressor-reverse osmosis de. *Renew. Energy* **2021**, *165*, 533–552. [CrossRef]
83. Calise, F.; Dentice d'Accadia, M.; Vanoli, R.; Vicidomini, M. Transient analysis of solar polygeneration systems including seawater desalination: A comparison between linear Fresnel and evacuated solar collectors. *Energy* **2019**, *172*, 647–660.
84. Ghorbani, B.; Ebrahimi, A.; Moradi, M.; Ziabasharhagh, M. Energy, exergy and sensitivity analyses of a novel hybrid structure for generation of Bio-Liquefied natural Gas, desalinated water and power using solar photovoltaic and geothermal source. *Energy Convers. Manag.* **2020**, *222*, 113215. [CrossRef]
85. Ghorbani, B.; Miansari, M.; Zendehboudi, S.; Hamedi, M.H. Exergetic and economic evaluation of carbon dioxide liquefaction process in a hybridized system of water desalination, power generation, and liquefied natural gas regasification. *Energy Convers. Manag.* **2020**, *205*, 112374. [CrossRef]
86. Vazini Modabber, H.; Khoshgoftar Manesh, M.H. 4E dynamic analysis of a water-power cogeneration plant integrated with solar parabolic trough collector and absorption chiller. *Therm. Sci. Eng. Prog.* **2021**, *21*, 100785. [CrossRef]
87. Sahoo, U.; Kumar, R.; Pant, P.C.; Chaudhary, R. Development of an innovative polygeneration process in hybrid solar-biomass system for combined power, cooling and desalination. *Appl. Therm. Eng.* **2017**, *120*, 560–567. [CrossRef]
88. Ghaebi, H.; Shekari Namin, A.; Rostamzadeh, H. Performance assessment and optimization of a novel multi-generation system from thermodynamic and thermoeconomic viewpoints. *Energy Convers. Manag.* **2018**, *165*, 419–439. [CrossRef]
89. Rostamzadeh, H.; Gargari, S.G.; Namin, A.S.; Ghaebi, H. A novel multigeneration system driven by a hybrid biogas-geothermal heat source, Part II: Multi-criteria optimization. *Energy Convers. Manag.* **2019**, *180*, 859–888. [CrossRef]
90. Abbasi, H.R.; Pourrahmani, H. Multi-criteria optimization of a renewable hydrogen and freshwater production system using HDH desalination unit and thermoelectric generator. *Energy Convers. Manag.* **2020**, *214*, 112903. [CrossRef]
91. Li, X.; Wang, Z.; Yang, M.; Yuan, G. Dynamic Simulation of a Novel Solar Polygeneration System for Heat, Power and Fresh Water Production based on Solar Thermal Power Tower Plant. *J. Therm. Sci.* **2020**, *29*, 378–392. [CrossRef]
92. El-Emam, R.S.; Dincer, I. Development and assessment of a novel solar heliostat-based multigeneration system. *Int. J. Hydrogen Energy* **2018**, *43*, 2610–2620. [CrossRef]

93. Rashidi, H.; Khorshidi, J. Exergoeconomic analysis and optimization of a solar based multigeneration system using multiobjective differential evolution algorithm. *J. Clean. Prod.* **2018**, *170*, 978–990. [CrossRef]
94. Islam, S.; Dincer, I.; Yilbas, B.S. Development, analysis and assessment of solar energy-based multigeneration system with thermoelectric generator. *Energy Convers. Manag.* **2018**, *156*, 746–756. [CrossRef]
95. Mouaky, A.; Rachek, A. Energetic, exergetic and exergeoeconomic assessment of a hybrid solar/biomass poylgeneration system: A case study of a rural community in a semi-arid climate. *Renew. Energy* **2020**, *158*, 280–296. [CrossRef]
96. Tan, R.R.; Aviso, K.B.; Foo, D.C.Y.; Lee, J.-Y.; Ubando, A.T. Optimal synthesis of negative emissions polygeneration systems with desalination. *Energy* **2019**, *187*, 115953. [CrossRef]
97. Siddiqui, O.; Dincer, I. A new solar and geothermal based integrated ammonia fuel cell system for multigeneration. *Int. J. Hydrogen Energy* **2020**, *45*, 34637–34653. [CrossRef]
98. Ayou, D.S.; Zaragoza, G.; Coronas, A. Small-scale renewable polygeneration system for off-grid applications: Desalination, power generation and space cooling. *Appl. Therm. Eng.* **2021**, *182*, 116112. [CrossRef]